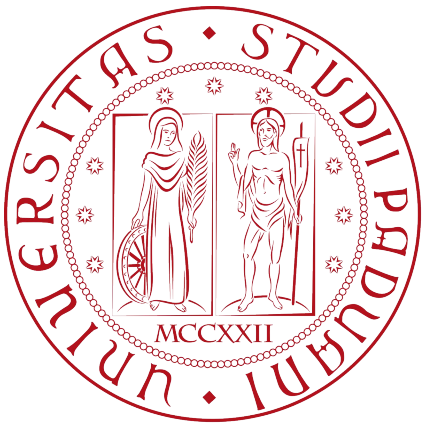

UNIVERSITÀ DEGLI STUDI DI PADOVA

Dipartimento di Fisica e Astronomia "Galileo Galilei"

Master Degree in Physics

Final Dissertation

Enhanced light quark Yukawa couplings

Thesis supervisor

Prof. Ramona Gröber

Candidate

Silvia Ziviani

Academic Year 2022/2023

Abstract

The end of the last millenium witnessed the triumph of the Standard Model (SM): the electroweak theory combined with quantum chromodynamics (QCD) provide an unified framework to describe three fundamental interactions of Nature, i.e. the electromagnetic, the weak and the strong interactions.
The discovery of the Higgs boson ten years ago has completed the SM, which has been extensively tested in the last decades. The high-precision measurements carried out at LEP, SLC, Tevatron, LHC and low energy high intensity experiments have firmly established that the SM provides the correct effective description of the strong and electroweak interactions at the currently reachable energies.
Nevertheless, some of the Higgs couplings remain for the moment nearly unconstrained. One example are the light quark Yukawa couplings. Current bounds and HL-LHC sensitivity studies show that the first generation quark Yukawa couplings can be constrained only up to several order of magnitude with respect to their Standard Model value.
In this Master thesis we investigate the possibility of building some concrete ultraviolet realisations providing large deviations in the light quarks Yukawa couplings.
To do that, we parameterize new physics (NP) contribution within the Standard Model effective field theory (SMEFT), and we focus on dimension six effective operators that can generate non-SM Yukawa-like terms. Once they are added to the SM Lagrangian, the Yukawa couplings get modified, in particular they can be enhanced by choosing appropriate NP parameters.
We choose to generate these effective operators at the high energy scale by introducing three new heavy vector-like quarks (VLQ), which interact with the SM particles and modify their couplings.
Matching the NP model to the SMEFT at the NP scale, we obtain bounds on the model parameters, namely the couplings of the VLQs to the SM particles and their mass, by confronting with bounds obtained from electroweak precision tests (EWPT) [1], flavour probes in particular for $\Delta F = 2$ processes [2] and Higgs Physics [3, 4].
In the light of the experimental bounds obtained on the UV parameters, we will finally show how large the enhancements of the light quark Yukawa couplings can be.
Those results will give a guideline which sensitivities should be obtained in experimental searches for light quark Yukawa couplings to probe realistic parameter space.

Contents

Chapter 1

The Standard Model

The Standard Model (SM) of particle physics provides the correct description of the strong and electroweak interactions at the currently reachable energies. It was developed by many scientists over the decades, nevertheless the main contributors can be identified as Weinberg, Glashow and Salam, whose original papers can be found in [5–7]. The SM is formulated as a quantum field theory and as any model of particle physics, it has to be constructed specifying:

- the gauge group G of the theory;
- the particle content of the theory;
- the possibility of spontaneous symmetry breaking of the group G into a smaller group G^{SSB}.

Let us introduce each ingredient.

1.1 Gauge group

The gauge group of a theory is the set of symmetries that underlie that theory's quantum field equations. The gauge group of the Standard Model is the product of three individual contributions, corresponding to the three fundamental forces described by the theory:

$$G_{SM} = SU(3)_c \otimes SU(2)_L \otimes U(1)_Y. \tag{1.1}$$

The symmetry group is local and as such gauged. We can immediately recognize two main sectors:

- **Strong interaction sector**: The strong interaction is described by the $SU(3)_c$ factor of the gauge group and it is mediated by particles called gluons. Gluons are massless, electrically neutral bosons that carry "color charge," which is the charge associated with the strong force.
- **Electroweak interaction sector**: The electroweak symmetry group, $SU(2)_L \otimes U(1)_Y$ is a combination of two separate symmetry groups: the first one is associated with the weak isospin force, while the second one is referred as the hypercharge.

At high energy scales the electroweak force is unified and mediated by the generator of the weak isospin and hypercharge gauge groups, namely three vector bosons W and one vector boson B, respectively. At the electroweak scale the SM symmetry group breaks into

$$G_{SM}^{SSB} = SU(3)_c \otimes U(1)_{em}. \tag{1.2}$$

While the strong sector stays untouched, the electroweak sector breaks into two distinct interactions: the weak interaction and the electromagnetic interaction. The first is mediated by three massive vector bosons ($W^{\pm}, Z$) while the second is mediated by the massless vector boson known as photon (γ).

1.2 Fields content

The SM contains all known elementary particles and their interactions. They can be divided into two categories: 1/2-spin particles (fermions) and integer-spin particles (bosons).

Fermions: Fermions are the building blocks of matter and come organized in three families called generations. Each fermion has both left- and right-handed components (except for neutrinos, which are only left-handed). The electroweak force is maximally parity violating, only the left-handed fermions couple to the $SU(2)$ gauge bosons. There are basically two kinds of fermions:

- The first kind of fermions are called quarks. They carry charge under the $SU(3)_c$ and as a consequence of this gauge interaction, they get bound into singlets of color charge called hadrons. There exist 6 different types of quarks, three of them with electric charge 2/3 (up, charm, top) and the other three with electric charge -1/3 (down, strange, and bottom). Their masses cover a very large range: they go from few MeV for the lightest ones (namely the up and down quarks, which are also the main constituents of matter since they form protons and neutrons) to the top quark, which with its 173 GeV mass is the heaviest particle of the SM [8].
- The second kind of fermions are called leptons. They are color singlets and, like quarks, there exist 6 particles. Three of them have a negative electric charge: the electron, the muon and the tau. In addition, there are three neutral and very light leptons called neutrinos. In the SM neutrinos are actually considered massless, while the charged lepton masses go from 511 keV (electron mass) to ~ 1.78 GeV (tau mass)[8].

Bosons: In the SM there are two categories of bosons fields:

- Gauge fields: These are spin-1 particles that mediate the interactions between fermions. In particular, they correspond to the generators of each symmetry group, whose number for a given $SU(N)$ group is $N^2 - 1$. In the electroweak sector we have the field B_μ which is associated to the generator of the $U(1)_Y$ group and three fields W^i_μ with $i = 1, 2, 3$ which are related to the generators of the $SU(2)_L$ group. In the strong interaction sector, the eight generators of the $SU(3)_c$ group are represented by an octet of fields G^a_μ with $a = 1, ..., 8$ called gluons.
- Higgs field: the last piece to complete the SM content is the Higgs field, which is a complex scalar field not charged under the color group but transforming in the fundamental representation of $SU(2)_L$ and carrying hypercharge $Y_\phi = 1/2$.
  The Higgs field plays a key role in the theory through the Spontaneous Symmetry Breaking (SSB) mechanism.

1.3 Higgs mechanism

Up to now, the gauge fields and the fermion fields have been kept massless. The reason is that the incorporation of explicit mass terms in the Lagrangian produces a manifest violation of the local $SU(2)_L \otimes U(1)_Y$ gauge invariance. However, we know from experiments that fermions and three of the gauge bosons are massive. How can we incorporate those masses into the SM without explicitly violating gauge invariance? The answer is provided by the Higgs-Brout-Englert mechanism, or just the Higgs mechanism for short [9–11].

The potential of the scalar field has a "Mexican hat-shape" (see figure 1.1), which means that its ground state is at value different from zero, i.e. it acquires a vacuum expectation value (vev), breaking the $SU(2)_L \otimes U(1)_Y$ symmetry and leaving a smaller $U(1)_{em}$ group unbroken. The Goldstone theorem states that for every spontaneously broken symmetry, the theory contains a number of massless scalar bosons (called Goldstone bosons) equal to the number of broken generators; in this case, as a net result three generators are broken. Those three would-be Goldstone bosons are absorbed by the new fields $W^\pm_\mu, Z_\mu$, becoming their longitudinal polarization. Thus, the weak physical bosons $W^\pm_\mu, Z_\mu$ become massive. Instead, the photon associated to the unbroken $U(1)_{em}$ symmetry remains massless.
The Higgs field is crucial also for the generation of the fermion masses, via the introduction of the Yukawa interaction, which is the main sector of interest for this thesis. For this reason, we will save

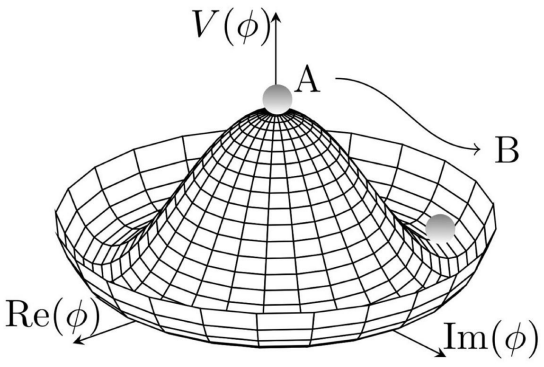

Figure 1.1: Representation of the mexican-hat potential of the Higgs field. The field configuration with minimal energy is not for a vanishing Higgs field (A) but for a non-vanishing vev of the Higgs field (B). The acquisition of this vev spontaneously breaks the symmetry.

its treatment for the next section.

1.4 The SM Lagrangian

1.4.1 Unbroken Lagrangian

The SM Lagrangian can be written in a compact form as

$$\mathcal{L}_{SM} = \mathcal{L}^{g.b.}_{kin} + \mathcal{L}^{f}_{kin} + \mathcal{L}^{\phi}_{kin} + \mathcal{L}^{\phi}_{pot} + \mathcal{L}_{Y}. \tag{1.3}$$

In particular:

- $\mathcal{L}^{g.b.}_{kin}$ is also called Yang-Mills term and contains all the kinetic terms of gauge bosons. Due to the non-abelian nature of the theory, it contains also interactions between gauge bosons,

$$\mathcal{L}^{g.b}_{kin} = -\frac{1}{4}G^{A\mu\nu}G^{A}_{\mu\nu} - \frac{1}{4}W^{I\mu\nu}W^{I}_{\mu\nu} - \frac{1}{4}B^{\mu\nu}B_{\mu\nu}, \tag{1.4}$$

  where the gauge boson field strength are defined as follows:

$$G^{A}_{\mu\nu} = \partial_\mu G^{A}_{\nu} - \partial_\nu G^{A}_{\mu} + g_3 f^{ABC} G^{B}_{\mu} G^{C}_{\nu}, \tag{1.5}$$
$$W^{I}_{\mu\nu} = \partial_\mu W^{I}_{\nu} - \partial_\nu W^{I}_{\mu} + g_2 \epsilon^{IJK} W^{J}_{\mu} W^{K}_{\nu}, \tag{1.6}$$
$$B_{\mu\nu} = \partial_\mu B_{\nu} - \partial_\nu B_{\mu}, \tag{1.7}$$

  with f^{ABC} and ϵ^{IJK} the structure constants of $SU(3)$ and $SU(2)$ respectively, defined by the commutation relations of the corresponding generators.

- $\mathcal{L}^{f}_{kin}$ is the gauge invariant kinetic term for matter fermions, which contains also the interactions between fermions and the gauge bosons.
  As said previously, the left-handed components of the fermions transform as doublets of $SU(2)_L$ while their right-handed components are singlets of $SU(2)_L$. For this reason, it's convenient to express the fields as follows:

$$Q^{i}_{L} = \begin{pmatrix} u^{i}_{L} \\ d^{i}_{L} \end{pmatrix}, \qquad u^{i}_{R}, d^{i}_{R}, \tag{1.8}$$
$$L^{i}_{L} = \begin{pmatrix} \nu^{i}_{L} \\ e^{i}_{L} \end{pmatrix}, \qquad e^{i}_{R}, \tag{1.9}$$

  where the index $i = 1, 2, 3$ runs over the three generations. In addition, all the quarks in the above equation have a color index that runs from 1 to 3, which is omitted for ease.

Finally, fermions are all carrying hypercharge, which is defined in terms of the third component of the weak isospin I_f^3 and the electric charge Q_f in units of the proton charge $(+e)$ as follows:

$$Y_f = Q_f - I_f^3. \tag{1.10}$$

So in particular we have:

$$Y_{Q_L^i} = 1/6, \qquad Y_{u_R^i} = 2/3, \qquad Y_{d_R^i} = -1/3, \tag{1.11}$$

$$Y_{L_L^i} = -1/2, \qquad Y_{e_R^i} = -1. \tag{1.12}$$

The kinetic term for fermions can be written in compact form as:

$$\mathcal{L}_{kin}^f = \sum_f \bar{\psi}_f i \not{D} \psi_f, \tag{1.13}$$

where we introduced the notation $\not{D} = \gamma^\mu D_\mu$ and the covariant derivative:

$$D_\mu = \partial_\mu - i g_3 \frac{\lambda^A}{2} W_\mu^A - i g_2 \frac{\sigma^I}{2} W_\mu^I - i g_1 Y_f B_\mu, \tag{1.14}$$

where λ^A with $A = 1, ..., 8$ are the Gell-Mann matrices (generators of the $SU(3)_c$), σ^I with $I = 1, 2, 3$ are the Pauli matrices (generators of the $SU(2)_L$), Y_f the hypercharge and g_1, g_2 and g_3 are the coupling constants of $U(1)_Y$, $SU(2)_L$ and $SU(3)_c$ respectively.

- $\mathcal{L}_{kin}^\phi$ is the kinetic term for the Higgs field:

$$\mathcal{L}_{kin}^\phi = (D_\mu \phi)^\dagger (D^\mu \phi). \tag{1.15}$$

This term contains the interactions between the Higgs field and the gauge bosons, and, remarkably, gives mass to the physical gauge bosons through the spontaneous symmetry breaking (SSB) mechanism.

- $\mathcal{L}_{pot}^\phi$ is the potential term for the Higgs field. Being a crucial ingredient for the Higgs mechanism, upon SSB it leads to a Higgs mass and Higgs self-interactions.

$$\mathcal{L}_{pot}^\phi = -V(\phi^\dagger \phi) = -\mu^2 \phi^\dagger \phi - \lambda (\phi^\dagger \phi)^2. \tag{1.16}$$

- $\mathcal{L}_Y$ is the Yukawa term. It generates the fermion masses and contains the Higgs interactions with fermions

$$\mathcal{L}_Y = \sum_f \bar{\psi}_f y_f \phi \psi_f, \tag{1.17}$$

where y_f is the Yukawa coupling of the fermion f.

Thus the renormalizable part of the SM Lagrangian invariant under the $G_{SM} = SU(3)_c \otimes SU(2)_L \otimes U(1)_Y$ assuming massless neutrinos is explicitly given by

$$\begin{aligned} \mathcal{L}_{SM} = & -\frac{1}{4} G^{A\mu\nu} G_{\mu\nu}^A - \frac{1}{4} W^{I\mu\nu} W_{\mu\nu}^I - \frac{1}{4} B^{\mu\nu} B_{\mu\nu} \\ & + (D_\mu \phi)^\dagger (D^\mu \phi) - \mu^2 \phi^\dagger \phi - \lambda (\phi^\dagger \phi)^2 \\ & + \sum_i \left[\bar{L}_L^i \not{D} L_L^i + \bar{Q}_L^i \not{D} Q_L^i + \bar{e}_R^i \not{D} e_R^i + \bar{u}_R^i \not{D} u_R^i + \bar{d}_R^i \not{D} d_R^i \right] \\ & - \sum_{ij} \left[\bar{L}_L^i y_e^{ij} \phi e_R^j + \bar{Q}_L^i y_d^{ij} \phi d_R^j + \bar{Q}_L^i y_u^{ij} (\tilde{\phi}) u_R^j + \text{h.c.} \right], \end{aligned} \tag{1.18}$$

where $\tilde{\phi} = i\sigma_2 \phi^*$ denotes the $SU(2)$ doublet of hypercharge $-1/2$.

1.4.2 Broken Lagrangian

As said previously, the electroweak gauge symmetry is broken once the Higgs field has acquired a vacuum expectation value. For the considered potential (1.16), the minimum is at

$$\langle\phi\rangle_0 = \langle 0|\phi|0\rangle = \left(-\frac{\mu^2}{2\lambda}\right)^{1/2} \equiv \frac{v}{\sqrt{2}}. \tag{1.19}$$

We expand the Higgs field around the vev, which at first order can be written in terms of four fields $\theta_{1,2,3}(x)$ and $h(x)$ as follows [12]:

$$\phi = \begin{pmatrix} \theta_2 + i\theta_1 \\ \frac{1}{\sqrt{2}}(v + h(x)) - i\theta_3 \end{pmatrix} = \frac{1}{\sqrt{2}} e^{i\theta_a(x)\sigma^a(x)/v} \begin{pmatrix} 0 \\ v + h(x) \end{pmatrix}. \tag{1.20}$$

It's now convenient to make a gauge transformation on this field to move to the so called unitary gauge:

$$\phi_{u.g.} = \frac{1}{\sqrt{2}} \begin{pmatrix} 0 \\ v + h(x) \end{pmatrix}. \tag{1.21}$$

Now we expand the kinetic term $|D_\mu\phi|^2$ of the Lagrangian and we define the new fields:

$$W^\pm_\mu = \frac{1}{\sqrt{2}}(W^1_\mu \mp iW^2_\mu), \qquad Z_\mu = \frac{g_2 W^3_\mu - g_1 B_\mu}{\sqrt{g_2^2 + g_1^2}}, \qquad A_\mu = \frac{g_2 W^3_\mu + g_1 B_\mu}{\sqrt{g_2^2 + g_1^2}}. \tag{1.22}$$

Each sector of the SM Lagrangian get modified after SSB, in particular:

- The bosonic sector in the unitary gauge reads

$$\begin{aligned} \mathcal{L}^{SSB}_{bos}|_{u.g.} = &-\frac{1}{4} G^{A\mu\nu} G^A_{\mu\nu} - \frac{1}{4} W^{I\mu\nu} W^I_{\mu\nu} - \frac{1}{4} B^{\mu\nu} B_{\mu\nu} \\ &+ \frac{1}{2}(\partial_\mu h)(\partial^\mu h) - \frac{1}{2} m_h^2 h^2 - \lambda v h^3 - \frac{\lambda}{4} h^4 \\ &+ \frac{(v+h)^2}{4} g_2^2 W^+_\mu W^{-\mu} + \frac{(v+h)^2}{2} \frac{(g_1^2 + g_2^2)}{4} Z_\mu Z^\mu. \end{aligned} \tag{1.23}$$

  Notice the appearence of the physical gauge boson mass terms:

$$M^2_{W^\pm} = \frac{(g_2 v)^2}{4}, \qquad M^2_Z = \frac{(g_1^2 + g_2^2)v^2}{4}. \tag{1.24}$$

- The fermionic sector in the unitary gauge reads

$$\mathcal{L}^{SSB}_f|_{u.g.} = \sum_f \bar{f}_L i\partial\!\!\!/ f_L + \sum_f \bar{f}_R i\partial\!\!\!/ f_R \qquad \text{Kinetic term} \tag{1.25}$$

$$- \frac{g_2}{\sqrt{2}}(W^-_\mu J^{+\mu} + W^+_\mu J^{-\mu}) \qquad \text{Weak CC} \tag{1.26}$$

$$- \frac{g_2}{c_W} Z_\mu J^\mu_Z \qquad \text{Weak NC} \tag{1.27}$$

$$- eA_\mu J^\mu_{em} \qquad \text{Electromagnetic current} \tag{1.28}$$

$$+ \mathcal{L}_Y, \qquad \text{Yukawa sector} \tag{1.29}$$

$$\tag{1.30}$$

  where the fermionic currents are:

$$J^-_\mu = \bar{u}_L \gamma_\mu d_L + \bar{\nu}_L \gamma_\mu e_L, \qquad J^+_\mu = \bar{d}_L \gamma_\mu u_L + \bar{e}_L \gamma_\mu \nu_L, \tag{1.31}$$

$$J^{em}_\mu = \sum_f Q_f \bar{f} \gamma_\mu f, \qquad J^Z_\mu = \sum_f \bar{f}_L \gamma_\mu I^3_f f_L + \sum_f Q_f \bar{f} \gamma_\mu f. \tag{1.32}$$

- The Yukawa sector in the unitary gauge becomes:

$$\mathcal{L}_Y|_{u.g.} = -\frac{v+h(x)}{\sqrt{2}}\left[\bar{u}^i_L y^{ij}_u u^j_R + \bar{d}^i_L y^{ij}_d d^j_R + \bar{e}^i_L y^{ij}_e e^j_R + \text{h.c.}\right], \tag{1.33}$$

where y^{ij}_f with $i,j = 1,2,3$ are 3×3 flavor mixing matrices.

1.4.3 Mass basis

In the following we will discuss further the Yukawa sector. Matter fields can be organized in triplets in flavor space:

$$u_{L,R} = \begin{pmatrix} u \\ c \\ t \end{pmatrix}_{L,R}, \qquad d_{L,R} = \begin{pmatrix} d \\ s \\ b \end{pmatrix}_{L,R}, \qquad e_{L,R} = \begin{pmatrix} e \\ \mu \\ \tau \end{pmatrix}_{L,R}. \tag{1.34}$$

The Yukawa matrices y^{ij}_f in (1.33) are generic 3×3 matrices in the interaction basis. The term with the vev in (1.33) gives a mass to the fermions. In order to have a consistent definition of the fermion masses, we would like to pass to the basis in which these matrices are diagonal. Let us rotate the fields:

$$\begin{cases} u'_L = L_u u_L \\ d'_L = L_d d_L \\ e'_L = L_e e_L \end{cases} \qquad \begin{cases} u'_R = R_u u_R \\ d'_R = R_d d_R \\ e'_R = R_e e_R \end{cases} \tag{1.35}$$

where the rotation matrices are all unitary:

$$LL^\dagger = L^\dagger L = \mathbb{1}, \qquad RR^\dagger = R^\dagger R = \mathbb{1}. \tag{1.36}$$

Performing these rotations the Yukawa sector Lagrangian becomes

$$\mathcal{L}_Y|_{u.g.} = -\frac{v+h(x)}{\sqrt{2}}\left[\bar{u}_L(L^\dagger_u L_u) y_u (R^\dagger_u R_u) u_R + \bar{d}_L(L^\dagger_d L_d) y_d (R^\dagger_d R_d) d_R + \bar{e}_L(L^\dagger_e L_e) y_e (R^\dagger_e R_e) e_R + \text{h.c.}\right] = \tag{1.37}$$

$$= -\frac{v+h(x)}{\sqrt{2}}\left[\bar{u}'_L(L_u y_u R^\dagger_u) u'_R + \bar{d}'_L(L_d y_d R^\dagger_d) d'_R + \bar{e}'_L(L_e y_e R^\dagger_e) e'_R + \text{h.c.}\right]. \tag{1.38}$$

It can be demonstrated that it is always possible to diagonalize a generic matrix by means of a biunitary transformation, so we can choose the R, L matrices such that

$$\hat{y}_f = L_f y_f R^\dagger_f = \begin{pmatrix} y_{f1} & & \\ & y_{f2} & \\ & & y_{f3} \end{pmatrix}. \tag{1.39}$$

Thus the fermion masses can be defined as

$$m^{ij}_f = \frac{v}{\sqrt{2}}\hat{y}^{ij}_f, \tag{1.40}$$

and in particular we have

$$m^{ij}_u = \begin{pmatrix} m_u & & \\ & m_c & \\ & & m_t \end{pmatrix}, \qquad m^{ij}_d = \begin{pmatrix} m_d & & \\ & m_s & \\ & & m_b \end{pmatrix}, \qquad m^{ij}_e = \begin{pmatrix} m_e & & \\ & m_\mu & \\ & & m_\tau \end{pmatrix}. \tag{1.41}$$

1.4.4 CKM Matrix

The change of basis (1.35) allows to obtain diagonal mass matrices, but can influence other interactions. Since the matrices L_f and R_f are unitary, the interactions involving the same type of fermions are not affected, so in particular the kinetic sector, the electromagnetic and the weak neutral interactions are still flavor diagonal in the mass basis. On the contrary, the weak charged interaction involves up-type and down-type fermions, so it is not possible to exploit the unitarity of the L_f matrices:

$$\mathcal{L}_{CC} = -\frac{g_2}{\sqrt{2}}\{\bar{u}'_L(L_u L_d^\dagger)\not{W}^+ d'_L + \bar{\nu}'_L(L_\nu L_e^\dagger)\not{W}^+ e'_L\}. \tag{1.42}$$

The matrix $L_u L_d^\dagger$ is called Cabibbo-Kobayashi-Maskawa (V_{CKM}) matrix [13], while the analogous matrix for leptons $L_\nu L_e^\dagger$ is called Pontecorvo-Maki-Sakata-Nakagawa (U_{PMSN}) matrix [14]. They are unitary matrices which have flavor mixing properties. Notice that if neutrinos are assumed to be massless, we can choose $L_\nu \equiv L_e$, so that $U_{PMSN} = \mathbb{1}$.

The matter content of the SM and its properties are summarized in the figure 1.2.

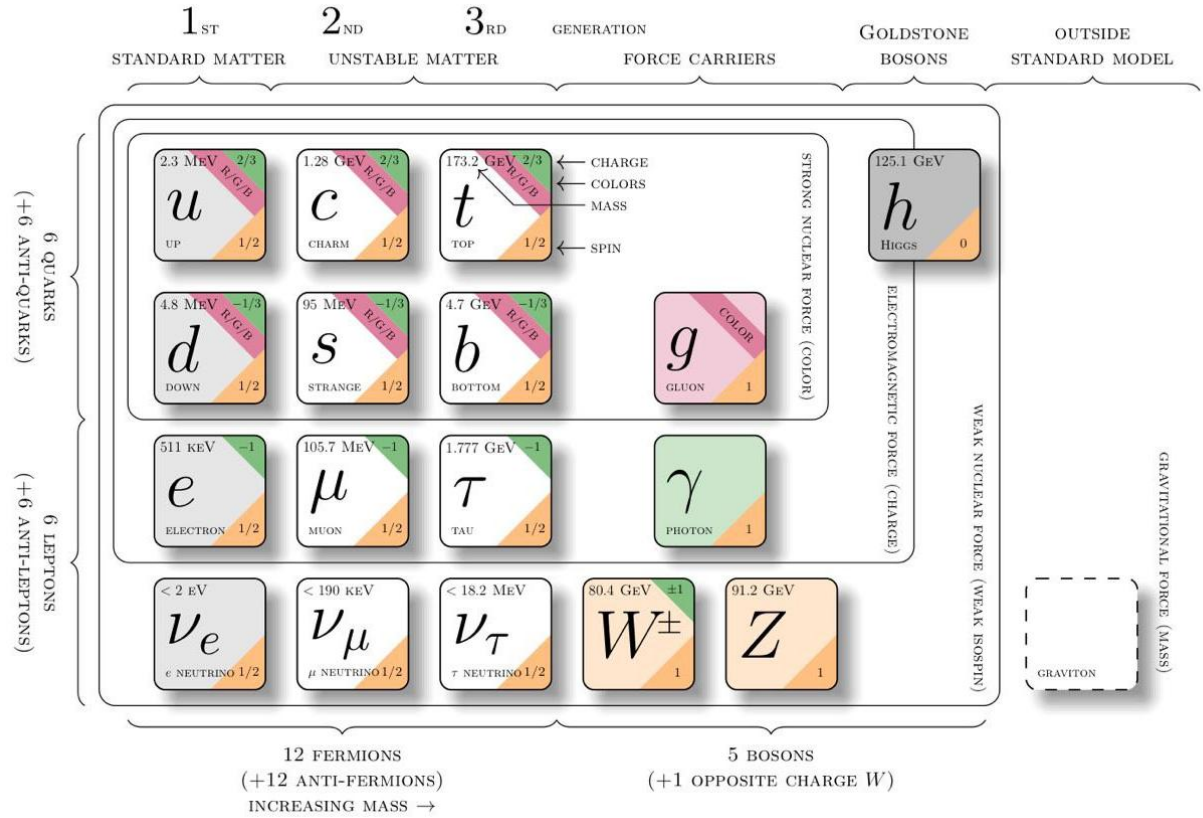

Figure 1.2: Summary of the SM field content. Schematically, on the left part three generations of fermions are shown, 6 quarks and 6 leptons. In the middle the force mediators are located, while in the upper right corner the Higgs boson is placed. All the fundamental properties (mass, electric charge, color charge, spin) are reported for each particle. Notice that particles are also organized in relation to which fundamental force they are involved in. In the lower right corner, not included in the SM framework, the graviton appears, which is thought to be the mediator of the gravitational force.

1.5 The Higgs couplings

More than ten years after the Higgs boson discovery at LHC [15], the properties of this particle are still to be fully understand, in particular its couplings to other SM particles. While the Higgs boson

couplings to gauge bosons and to third generation fermions have been measured at the $\mathcal{O}(5-20)\%$ level [3, 4], the Higgs boson couplings to the first two generations and the Higgs self-couplings remain more elusive.

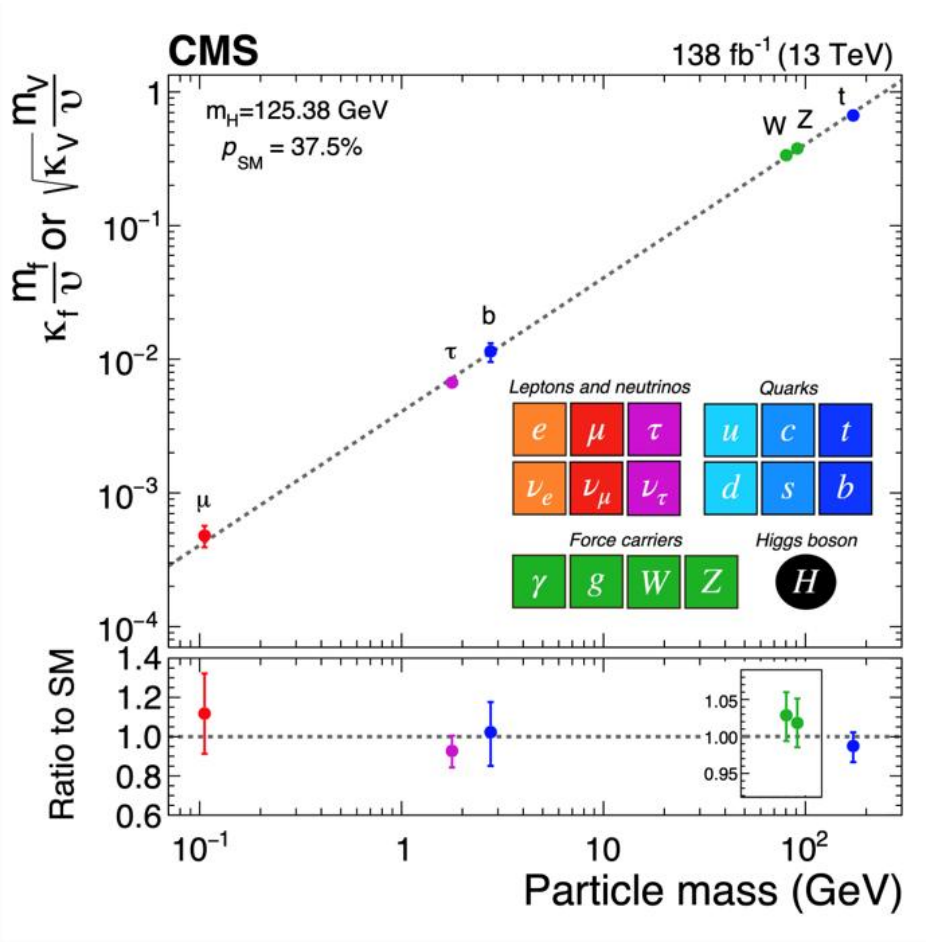

Figure 1.3: State-of-the-art of the Higgs couplings to the SM particles [16]. Upper plot: on the vertical axis, the SM prediction multiplied by a κ-parameter is shown, while the horizontal axis shows the particle mass in GeV. Lower plot: the ratio to the SM is given as a function of the particle mass. The couplings to heavy fermions and gauge bosons are well measured and in great agreement with their SM expectation, but the absence of light quark couplings catches the eye.

To study possible deviations from the SM induced by new physics, the so called κ-framework has been introduced, which is described in details in [17, 18]. The value of κ parameterizes a potential deviation of the Higgs couplings with respect to their SM values as follows:

$$\kappa_i = \frac{g_{hi}}{g_{hi}^{SM}}. \tag{1.43}$$

Figure 1.3 from the CMS collaboration [16] shows the state-of-the-art of the Higgs couplings measurements. Remarkably, the Higgs boson couplings to gauge bosons and heavy fermions have been measured very precisely and they are in wonderful agreement with their SM predictions, however the absence of the Higgs couplings to light fermions stands out. The reason is that, according to the Higgs mechanism of SM, the Yukawa couplings of the fermions are proportional to the ratio between their mass and the Higgs vev, namely:

$$y_f \propto \frac{m_f}{v}, \qquad \text{with } v = 246 \text{ GeV}. \tag{1.44}$$

In particular, for the light fermions the ratio m_f/v is vanishingly small, and hence the scattering processes involving their interaction with the Higgs boson are so strongly suppressed that they are in

practice unobservable in the SM. Moreover, in the quark case their production is immediately followed by hadronization, so they appear as (quasi) indistinguishable jets in the detector. On the other hand, there exist various proposal on how to constrain the light Yukawa couplings exploiting measurements of specific processes. For the charm quark, for instance, the Vh production with subsequent decay $h \to c\bar{c}$ and Higgs+charm production processes can be exploited [19–21], but also exclusive Higgs decays to vector mesons can be used to constrain the charm Yukawa coupling [22–25]. For the strange quark the Yukawa coupling constraining is more challenging, but there are some proposals for strange tagging at lepton colliders [26].
For the first quark generation a different approach is needed since the Higgs decays to light quarks cannot be measured directly. Some constraints can be obtained by exploiting the fact that for enhanced light quark Yukawa couplings, a significant contribution to the Higgs production can come from processes in which the Higgs boson couples directly to the quark content of the parton distribution, which in the case of protons is dominated by up and down quarks. In this sense one can use processes like Higgs+γ [27], Higgs+jet [28, 29], Higgs pair production [30, 31], tri-vector boson production [32, 33] and the charge asymmetry in $W^{\pm}h$ [34, 35]. Even at the high-luminosity LHC (HL-LHC) the constraints remain quite relaxed: in a global fit the following limits were found [36]

$$\kappa_u < 560, \qquad \kappa_c < 1.2, \tag{1.45}$$

$$\kappa_d < 260, \qquad \kappa_s < 13. \tag{1.46}$$

A recent study [37] has shown that, using kinematic discriminants in the analysis of the Higgs off-shell production, the up and down Yukawa couplings can be further constrained at the HL-LHC (assuming only experimental systematic uncertainties):

$$\kappa_u < 260, \qquad \kappa_d < 156. \tag{1.47}$$

This is a considerable improvement, but nevertheless these couplings can be constrained only up to several order of magnitude with respect to their SM values. Thus the question, which motivated this work, is the following: **is it possible to build a new physics (NP) model, consistent with all the current experimental bounds, in which these light quark Yukawa couplings are largely enhanced?**
The aim of this Master's thesis is exactly to investigate this possibility. The first step is to identify the best approach to parameterize NP effects in a handy and theoretically consistent way.
The best choice is to adopt an effective field theory description, since it is a model-independent and theoretical consistent framework. Indeed, the κ parameterization is not gauge invariant and does not allow for new Lorentz structures. Nevertheless, constraints derived in the κ analysis can be directly exploited to put constraints on NP parameters, as will be discussed in chapter 5.

Chapter 2

Effective Field Theory

2.1 A very powerful tool

Effective field theories have in the past proven to be very useful tools. For instance, we can describe the motion of an apple falling off a tree without the exact knowledge of the dynamics of the atoms in the apple.
The same holds true for the SM which can be regarded as an effective field theory up to some scale $\Lambda \gg v$, where Λ cannot be larger as the Planck scale where gravitational interactions will be relevant. In order to advance in our understanding of fundamental interactions, we can proceed through a direct discovery of a new particle or indirectly. Crucially, the information gathered through indirect methods have historically directed the search for a new particle or new theoretical framework. A striking example was the construction of the Large Hadron Collider (LHC), which was based on the expectation that the SSB mechanism $SU(2)_L \otimes U(1)_Y \to U(1)_{em}$ would be revealed by probing the TeV energy range. As known, this expectation has been met to date with the discovery of the Higgs boson in July 2012, which completed the SM framework. Since then, the SM predictions have been extensively tested, giving an astonishing agreement between theory and experiments. In the last years, the lack of statistically significant deviations in the global data set has suggested that there is a gap between the electroweak scale and the new physics scale. This fact at the same time motivates:

- the upgrade of experimental facilities (e.g. HL-LHC) to improve statistically marginal measurements;
- an increasing understanding of the SM to improve theoretical predictions;
- the sharpening of our theoretical tools to indirectly search for physics beyond the SM.

Effective field theories have been proven in the last few years as a useful tool to parameterise our ignorance of the possible UV dynamics.
The general idea is to use field theories to describe Physics at low energy (or, equivalently, at long distances) even if we don't know the ultimate, complete theory. In short, an EFT provides an effective description of physics up to a certain energy scale Λ (in jargon "cutoff"), which represents a "threshold of ignorance" beyond which not included physics comes into play.
The main advantage of EFT is that it allows to study large sets of experimental data without the claim to be valid to arbitrarily high energies. Despite being non renormalizable theories, the EFT utilities are remarkable:

- Firstly, EFTs can be very useful even when the complete theory is known: for instance, the full theory could be quite complicated and passing to an EFT could simplify things greatly. In this case, the EFT can be constructed from its UV completion by simply integrating out its heavy degrees of freedom. This can be done in two ways: through the effective action S_{eff} or manipulating the equation of motion. The result is a theory with a limited range of applicability, but much more handy in that range than the corresponding complete theory.
- The power of EFT emerges in all its glory especially in the exploration of new physics models

that could extend the SM: they provide a theoretical well-defined framework with an ordering to describe model-independently NP.

Overall, EFTs are a valuable tool in theoretical physics, providing a pragmatic and flexible approach to studying physical systems, particularly when dealing with different energy scales and degrees of complexity. It allows physicists to effectively model and understand various phenomena without having to resort to the full complexity of the underlying theories.
The concept of EFT has a rich history and is extensively employed in many fields of Physics: Gravity Physics (e.g. GEFT = Gravitational EFT), Cosmology (EFT of Inflation), Material Physics (EMT = Effective Medium Theory), Nuclear and Atomic Physics (NRQFT=non relativistic QFT), Electromagnetism, neutrino Physics and many others.
In the 1980s and beyond, EFT became increasingly relevant in particle physics, for instance the Fermi Theory of β Decay [38], Low Energy Field Theory(LEFT) [39, 40], Chiral Perturbation Theory (ChPT) [41, 42] and Heavy Quark Effective Theory (HQET) [43].
In the Higgs Physics context, the main EFT of interest are the Standard Model effective field theory (SMEFT) and the Higgs effective field theory (HEFT). The main difference between the two is that the former assumes that the scalar field transforms as a $SU(2)_L$ doublet, while in the latter this assumption is lifted. In this work we make use of the SMEFT framework, which will be discussed in section 2.2. For the treatment of HEFT we suggest the reading of [44].

2.2 SMEFT

The SMEFT provides a simple and well-defined model-independent framework to study NP beyond the SM. For an extensive treatment of SMEFT see for instance [44]. Being an effective field theory, SMEFT is only valid at energies below the threshold of production of any extra degrees of freedom. It provides a parameterization of the NP effects preserving the SM gauge group. The SMEFT which follows from this assumption is defined as:

$$\mathcal{L}_{SMEFT} = \mathcal{L}_{SM} + \mathcal{L}^{(5)} + \mathcal{L}^{(6)} + \mathcal{L}^{(7)} + ... \tag{2.1}$$

where the general term is defined as:

$$\mathcal{L}^{(d)} = \sum_{i=1}^{n_d} \frac{C_i^d}{\Lambda^{d-4}} Q_i^d, \qquad \text{for } d > 4. \tag{2.2}$$

The Q_i^d are higher dimensional operators, each suppressed by $d-4$ powers of the cutoff scale Λ, while the C_i^d are dimensionless coupling constants called Wilson coefficients. Remarkably, not all the operators Q_i^d are independent: by exploiting algebraic identities and field redefinitions, certain linear combinations can be removed from $\mathcal{L}_{SMEFT}$.
Due to the suppression factor of powers of the cutoff Λ, the most relevant effective contributions to the SM Lagrangian turn out to be the new "lowest" dimensions terms.
Let us start considering $\mathcal{L}^{(5)}$: the dimension-5 operators involve the lepton number violation ($\Delta L = 2$) and its Hermitian conjugate ($\Delta L = -2$). These operators are relevant for processes involving neutrino masses and oscillations, but they do not affect the Higgs interactions. On the other hand, the dimension-6 operators in SMEFT are the first ones that become important for collider physics at energies beyond the electroweak scale. For this reason, we shall start directly considering dimension-6 operators. Although the number of non-redundant operators in $\mathcal{L}^{(6)}$ was known [45], it took more than twenty years to obtain a complete non redundant operator basis for $\mathcal{L}^{(6)}$. In the next section the most famous dimension-6 operator basis is reported.

2.2.1 A non redundant 6-dim operator basis: the Warsaw basis

In this work we choose the first non-redundant operator basis for $\mathcal{L}^{(6)}$ determined in [46], which is known in literature as the "Warsaw basis". Assuming baryon number conservation, Rosiek *et al.*

found 59 independent operators (barring flavour structure and Hermitian conjugations), compared to the 80 operators listed in [45].
To obtain a non-redundant basis it is necessary to employ field redefinitions, Fierz identities and partial integration. To find all the gauge-invariant operators is sufficient to impose the $SU(3)_c \otimes SU(2)_L \otimes U(1)_Y$ gauge invariance and use as building blocks:

- the matter fields l^j_{Lp}, e_{Rp}, $q^{\alpha j}_{Lp}$, u^{α}_{Rp}, d^{α}_{Rp}, ϕ^j (with p =generation index, $j = SU(2)_L$ index, α =color index);
- the field strength tensors $X_{\mu\nu} \in G^A_{\mu\nu}, W^I_{\mu\nu}, B_{\mu\nu}$;
- covariant derivatives D of these objects.

The complete basis is reported in tables 2.1,2.2, where for sake of simplicity we dropped the chiral subscript with respect to (1.8). Notice also that the indices p, r, s, t are generations indices of the fermion fields, to be supplemented when needed (e.g. $Q_{ll} \to Q^{prst}_{ll}$).

X^3		ϕ^6 and $\phi^4 D^2$		$\psi^2\phi^3$	
Q_G	$f^{ABC} G^{A\nu}_{\mu} G^{B\rho}_{\nu} G^{C\mu}_{\rho}$	Q_ϕ	$(\phi^\dagger\phi)^3$	$Q_{e\phi}$	$(\phi^\dagger\phi)(\bar{L}_p e_r \phi)$
$Q_{\tilde{G}}$	$f^{ABC} \tilde{G}^{A\nu}_{\mu} G^{B\rho}_{\nu} G^{C\mu}_{\rho}$	$Q_{\phi\Box}$	$(\phi^\dagger\phi)\Box(\phi^\dagger\phi)$	$Q_{u\phi}$	$(\phi^\dagger\phi)(\bar{Q}_p u_r \tilde{\phi})$
Q_W	$\epsilon^{IJK} W^{I\nu}_{\mu} W^{J\rho}_{\nu} W^{K\mu}_{\rho}$	$Q_{\phi D}$	$(\phi^\dagger D^\mu \phi)^*(\phi^\dagger D_\mu \phi)$	$Q_{d\phi}$	$(\phi^\dagger\phi)(\bar{Q}_p d_r \phi)$
$Q_{\tilde{W}}$	$\epsilon^{IJK} \tilde{W}^{I\nu}_{\mu} W^{J\rho}_{\nu} W^{K\mu}_{\rho}$				
$X^2\phi^2$		$\psi^2 X\phi$		$\psi^2\phi^2 D$	
$Q_{\phi G}$	$\phi^\dagger\phi G^A_{\mu\nu} G^{A\mu\nu}$	Q_{eW}	$(\bar{L}_p\sigma^{\mu\nu} e_r)\sigma^I \phi W^I_{\mu\nu}$	$Q^{(1)}_{\phi l}$	$(\phi^\dagger i \overleftrightarrow{D}_\mu \phi)(\bar{L}_p\gamma^\mu L_r)$
$Q_{\phi\tilde{G}}$	$\phi^\dagger\phi \tilde{G}^A_{\mu\nu} G^{A\mu\nu}$	Q_{eB}	$(\bar{L}_p\sigma^{\mu\nu} e_r)\phi B_{\mu\nu}$	$Q^{(3)}_{\phi l}$	$(\phi^\dagger i \overleftrightarrow{D}^I_\mu \phi)(\bar{L}_p\sigma^I\gamma^\mu L_r)$
$Q_{\phi W}$	$\phi^\dagger\phi W^I_{\mu\nu} W^{I\mu\nu}$	Q_{uG}	$(\bar{Q}_p\sigma^{\mu\nu} u_r)T^A\tilde{\phi} G^A_{\mu\nu}$	$Q_{\phi e}$	$(\phi^\dagger i \overleftrightarrow{D}_\mu \phi)(\bar{e}_p\gamma^\mu e_r)$
$Q_{\phi\tilde{W}}$	$\phi^\dagger\phi \tilde{W}^I_{\mu\nu} W^{I\mu\nu}$	Q_{uW}	$(\bar{Q}_p\sigma^{\mu\nu} u_r)\sigma^I\tilde{\phi} W^I_{\mu\nu}$	$Q^{(1)}_{\phi q}$	$(\phi^\dagger i \overleftrightarrow{D}_\mu \phi)(\bar{Q}_p\gamma^\mu Q_r)$
$Q_{\phi B}$	$\phi^\dagger\phi B_{\mu\nu} B^{\mu\nu}$	Q_{uB}	$(\bar{Q}_p\sigma^{\mu\nu} u_r)\tilde{\phi} B_{\mu\nu}$	$Q^{(3)}_{\phi q}$	$(\phi^\dagger i \overleftrightarrow{D}^I_\mu \phi)(\bar{Q}_p\sigma^I\gamma^\mu Q_r)$
$Q_{\phi\tilde{B}}$	$\phi^\dagger\phi \tilde{B}_{\mu\nu} B^{\mu\nu}$	Q_{dG}	$(\bar{Q}_p\sigma^{\mu\nu} d_r)T^A\phi G^A_{\mu\nu}$	$Q_{\phi u}$	$(\phi^\dagger i \overleftrightarrow{D}_\mu \phi)(\bar{u}_p\gamma^\mu u_r)$
$Q_{\phi WB}$	$\phi^\dagger\sigma^I\phi W^I_{\mu\nu} B^{\mu\nu}$	Q_{dW}	$(\bar{Q}_p\sigma^{\mu\nu} d_r)\sigma^I\phi W^I_{\mu\nu}$	$Q_{\phi d}$	$(\phi^\dagger i \overleftrightarrow{D}_\mu \phi)(\bar{d}_p\gamma^\mu d_r)$
$Q_{\phi\tilde{W}B}$	$\phi^\dagger\sigma^I\phi \tilde{W}^I_{\mu\nu} B^{\mu\nu}$	Q_{dB}	$(\bar{Q}_p\sigma^{\mu\nu} d_r)\phi B_{\mu\nu}$	$Q_{\phi ud}$	$(\tilde{\phi}^\dagger i \overleftrightarrow{D}_\mu \phi)(\bar{u}_p\gamma^\mu d_r)$

Table 2.1: Basis of dimension-six operators other than four-fermion interactions.

Let's briefly describe each kind of operators, starting from the bosonic ones.

Bosonic operators Purely bosonic operators should contain an even number of Higgs field ϕ (because of the constraints on the $SU(2)_L$ tensor product) and an even number of covariant derivatives (to contract all the Lorentz indices). Moreover, since the mass dimension of ϕ and D is 1, while for the strength tensor X is 2, no dimension 5 operators can emerge in the bosonic sector. The possibilities for the dimension 6 bosonic operator field are: X^3, ϕ^6, $\phi^4 D^2$, $\phi^2 D^4$, $\phi^2 X D^2$, $X^2 D^2$. Actually it is possible to demonstrate that the last three reduce by the equations of motion (EoMs) either to the former classes or to operators containing fermions. This is the reason why they do not appear in table 2.1.

Single-fermionic-current operators The non redundant single-fermionic-current operators can be divided in three classes:

- $\psi^2\phi^3$: Since the fermion current must be an isospin doublet and color singlet of the form $\bar{\psi}_i\psi_j$, the only possibilities for this class are the Yukawa terms multiplied by $\phi^\dagger\phi$. Notice that the number of conjugated and unconjugated scalar fields in ϕ^3 is set by hypercharge constraints.
- $\psi^2 X\phi$: In this case the Higgs field and the antisymmetric tensor require an isospin doublet of the form $\bar{\psi}_i\sigma^{\mu\nu}\psi_j$. The Higgs field combines to the fermion current analogously to the standard Yukawa terms, while the tensors $W^I_{\mu\nu}$ and $G^A_{\mu\nu}$ need to be contracted with isospin triplets and color octects respectively.

$(\bar{L}L)(\bar{L}L)$		$(\bar{R}R)(\bar{R}R)$		$(\bar{L}L)(\bar{R}R)$	
Q_{ll}	$(\bar{L}_p\gamma_\mu L_r)(\bar{L}_s\gamma^\mu L_t)$	Q_{ee}	$(\bar{e}_p\gamma_\mu e_r)(\bar{e}_s\gamma^\mu e_t)$	Q_{le}	$(\bar{L}_p\gamma_\mu L_r)(\bar{e}_s\gamma^\mu e_t)$
$Q_{qq}^{(1)}$	$(\bar{Q}_p\gamma_\mu Q_r)(\bar{Q}_s\gamma^\mu Q_t)$	Q_{uu}	$(\bar{u}_p\gamma_\mu u_r)(\bar{u}_s\gamma^\mu u_t)$	Q_{lu}	$(\bar{L}_p\gamma_\mu L_r)(\bar{u}_s\gamma^\mu u_t)$
$Q_{qq}^{(3)}$	$(\bar{Q}_p\gamma_\mu\sigma^I Q_r)(\bar{Q}_s\gamma^\mu\sigma^I Q_t)$	Q_{dd}	$(\bar{d}_p\gamma_\mu d_r)(\bar{d}_s\gamma^\mu d_t)$	Q_{ld}	$(\bar{L}_p\gamma_\mu L_r)(\bar{d}_s\gamma^\mu d_t)$
$Q_{lq}^{(1)}$	$(\bar{L}_p\gamma_\mu L_r)(\bar{Q}_s\gamma^\mu Q_t)$	Q_{eu}	$(\bar{e}_p\gamma_\mu e_r)(\bar{u}_s\gamma^\mu u_t)$	Q_{qe}	$(\bar{Q}_p\gamma_\mu Q_r)(\bar{e}_s\gamma^\mu e_t)$
$Q_{lq}^{(3)}$	$(\bar{L}_p\gamma_\mu\sigma^I L_r)(\bar{Q}_s\gamma^\mu\sigma^I Q_t)$	Q_{ed}	$(\bar{e}_p\gamma_\mu e_r)(\bar{d}_s\gamma^\mu d_t)$	$Q_{qu}^{(1)}$	$(\bar{Q}_p\gamma_\mu Q_r)(\bar{u}_s\gamma^\mu u_t)$
		$Q_{ud}^{(1)}$	$(\bar{u}_p\gamma_\mu u_r)(\bar{d}_s\gamma^\mu d_t)$	$Q_{qu}^{(8)}$	$(\bar{Q}_p\gamma_\mu T^A Q_r)(\bar{u}_s\gamma^\mu T^A u_t)$
		$Q_{ud}^{(8)}$	$(\bar{u}_p\gamma_\mu T^A u_r)(\bar{d}_s\gamma^\mu T^A d_t)$	$Q_{qd}^{(1)}$	$(\bar{Q}_p\gamma_\mu Q_r)(\bar{d}_s\gamma^\mu d_t)$
				$Q_{qd}^{(8)}$	$(\bar{Q}_p\gamma_\mu T^A Q_r)(\bar{d}_s\gamma^\mu T^A d_t)$

$(\bar{L}R)(\bar{R}L)$ and $(\bar{L}R)(\bar{L}R)$		B-violating	
Q_{ledq}	$(\bar{L}_p^j e_r)(\bar{d}_s Q_t^j)$	Q_{duq}	$\epsilon^{\alpha\beta\gamma}\epsilon_{jk}\,[(d_p^\alpha)^T C u_r^\beta]\,[(Q_s^{\gamma j})^T C L_t^k]$
$Q_{quqd}^{(1)}$	$(\bar{Q}_p^j u_r)\epsilon_{jk}(\bar{Q}_s^k d_t)$	Q_{qqu}	$\epsilon^{\alpha\beta\gamma}\epsilon_{jk}\,[(Q_p^{\alpha j})^T C Q_r^{\beta k}]\,[(u_s^\gamma)^T C e_t]$
$Q_{quqd}^{(8)}$	$(\bar{Q}_p^j T^A u_r)\epsilon_{jk}(\bar{Q}_s^k T^A d_t)$	Q_{qqq}	$\epsilon^{\alpha\beta\gamma}\epsilon_{jn}\epsilon_{km}\,[(Q_p^{\alpha j})^T C Q_r^{\beta k}]\,[(Q_s^{\gamma m})^T C L_t^n]$
$Q_{legd}^{(1)}$	$(\bar{L}_p^j u_r)\epsilon_{jk}(\bar{Q}_s^k u_t)$	Q_{duu}	$\epsilon^{\alpha\beta\gamma}\,[(d_p^\alpha)^T C u_r^\beta]\,[(u_s^\gamma)^T C e_t]$
$Q_{legd}^{(3)}$	$(\bar{L}_p^j\sigma_{\mu\nu} e_r)\epsilon_{jk}(\bar{Q}_s^k\sigma^{\mu\nu} u_t)$		

Table 2.2: Basis of dimension-six operators for four-fermion interactions.

- $\psi^2\phi^2 D$: When the derivative acts on any of the fermion field, its contraction with the fermionic current produces EoMs which leads to the already discussed class $\psi^2\phi^3$, so it's sufficient to consider the cases in which derivatives act on the scalars only. Hermitianity requires the presence of $\overleftrightarrow{D}_\mu \equiv D_\mu - \overleftarrow{D}_\mu$, which explicity leads to terms like:

$$\phi^\dagger i\overleftrightarrow{D}_\mu\phi = i\phi^\dagger(D_\mu\phi) - i(D_\mu\phi)^\dagger\phi. \tag{2.3}$$

Four-fermion operators This class of operators can be further classified in $(\bar{L}L)(\bar{L}L)$,$(\bar{R}R)(\bar{R}R)$, $(\bar{L}L)(\bar{R}R)$,$(\bar{L}R)(\bar{R}L)$ and $(\bar{L}R)(\bar{L}R)$), plus four $B-$violating operators. They are all collected in table 2.2.

2.3 Light Yukawa couplings in EFT

In this work we are interested in an enhancement of the Yukawa couplings. In [47] a complete set of Feynman rules for the SMEFT is given. In particular, the quark-Higgs vertices receive a contribution from the following dimension-six operators appearing in tables 2.1,2.2: $Q_{\phi\Box}$, $Q_{\phi D}$, $Q_{u\phi}$ and $Q_{d\phi}$.
The first two operators require a redefinition of the Higgs field to have canonical normalised kinetic terms and lead to a general shift of the Higgs couplings. Their contributions thus affect also other Higgs couplings, so they can be constrained exploiting for instance Higgs couplings to vector bosons, which are experimentally much better constrained than light Yukawa couplings. For this reason, we just consider the operators:

$$Q_{u\phi} = (\phi^\dagger\phi)(\bar{Q}_p u_r\tilde{\phi}), \tag{2.4}$$

$$Q_{d\phi} = (\phi^\dagger\phi)(\bar{Q}_p d_r\phi). \tag{2.5}$$

The new Yukawa sector becomes:

$$\mathcal{L}_{Y+NP} = \bar{Q}_L^i y_d^{ij}\phi d_R^j + \bar{Q}_L^i y_u^{ij}\tilde{\phi}u_R^j - \frac{(\phi^\dagger\phi)}{\Lambda^2}\left(\bar{Q}_L^i C_{d\phi}^{ij}\phi d_R^j + \bar{Q}_L^i C_{u\phi}^{ij}\tilde{\phi}u_R^j + \right) + \text{h.c.} \tag{2.6}$$

Let us pass to the unitary gauge:

$$\mathcal{L}_{Y+NP|_{u.g.}} = \frac{v+h}{\sqrt{2}}\left(\bar{d}_L^i y_d^{ij} d_R^j + \bar{u}_L^i y_u^{ij} u_R^j\right) - \frac{v+h}{\sqrt{2}}\frac{(v+h)^2}{2\Lambda^2}\left(\bar{d}_L^i C_{d\phi}^{ij} d_R^j + \bar{u}_L^i C_{u\phi}^{ij} u_R^j + \right) + \text{h.c.} \tag{2.7}$$

Therefore, the mass matrices of the up-type and down-type quarks get modified as follows:

$$M_q^{ij} = \frac{v}{\sqrt{2}}\big(y_q^{ij} - \frac{v^2}{2\Lambda^2}C_{q\phi}^{ij}\big), \qquad \text{with } q = u, d. \tag{2.8}$$

This modification of the mass matrix implies a modification of the rotation matrices (1.35) which allow to pass from the interaction basis to the mass eigenbasis:

$$m_f^{ij} = \frac{v}{\sqrt{2}}L'_f\big(y_q^{ij} - \frac{v^2}{2\Lambda^2}C_{q\phi}^{ij}\big)(R'_f)^\dagger. \tag{2.9}$$

In the mass basis we denote the Wilson coefficients as:

$$(\tilde{C}_{q\phi})_{ij} = \big(L'_f C_{q\phi}(R'_f)^\dagger\big)_{ij}. \tag{2.10}$$

The Lagrangian in the mass basis now reads:

$$\mathcal{L}_{Y+NP}|_{m.b.} = \frac{v+h}{\sqrt{2}}\big(\bar{d}'_L\hat{y}_d d'_R + \bar{u}'_L\hat{y}_u u'_R\big) - \frac{v+h}{\sqrt{2}}\frac{(v+h)^2}{2\Lambda^2}\big(\bar{d}'_L\tilde{C}_{d\phi}d'_R + \bar{u}'_L\tilde{C}_{u\phi}u'_R\big) + \text{h.c.} \tag{2.11}$$

$$= \frac{v+h}{\sqrt{2}}\big[m_{q_i}\bar{q}_i q_j\delta_{ij} + \frac{v^2}{2\Lambda^2}\bar{q}_i(\tilde{C}_{q\phi})_{ij}q_j - \frac{v^2+2vh+h^2}{2\Lambda^2}\bar{q}_i(\tilde{C}_{q\phi})_{ij}q_j\big] + \text{h.c.} \tag{2.12}$$

$$= \frac{v+h}{\sqrt{2}}\big[m_{q_i}\bar{q}_i q_j\delta_{ij} - \frac{vh}{\Lambda^2}\bar{q}_i(\tilde{C}_{q\phi})_{ij}q_j - \frac{h^2}{2\Lambda^2}\bar{q}_i(\tilde{C}_{q\phi})_{ij}q_j\big] + \text{h.c.} \tag{2.13}$$

where in the last two rows q_i with flavor index $i = 1, 2, 3$ and $q = u, d$ are the quark fields in the mass basis.

From equation (2.13) the couplings of the Higgs boson to quarks are immediately derived:

$$g_{hq_i\bar{q}_j} = \frac{m_q}{v}\delta_{ij} - \frac{1}{\sqrt{2}}\frac{v^2}{\Lambda^2}(\tilde{C}_{q\phi})_{ij}, \quad g_{hhq_i\bar{q}_j} = -\frac{3}{2\sqrt{2}}\frac{v}{\Lambda^2}(\tilde{C}_{q\phi})_{ij}, \quad g_{hhhq_i\bar{q}_j} = -\frac{1}{2\sqrt{2}}\frac{1}{\Lambda^2}(\tilde{C}_{q\phi})_{ij}. \tag{2.14}$$

Chapter 3

UV model

The aim of this thesis is to construct a model in which the large enhancements of the Yukawa couplings are concretely realized. To do that, we need to introduce new degrees of freedom, namely new particles, which arise at high energy scales, and whose interactions with the SM particles can have effects on the Yukawa couplings.
While in principle there exist an infinite amount of theories one should follow certain guidelines in order to stay consistent with experimental observations. Given the consistency of the SM with all experimental measurements so far the following guidelines should be used:

1. At energy scales below a certain cutoff Λ, Nature is well described by a four-dimensional Poincaré-invariant local effective Lagrangian $\mathcal{L}_{BSM}$.
2. $\mathcal{L}_{BSM}$ includes as a subset all the fields appearing in the SM and they have the same transformation rules under the SM gauge group.
3. $\mathcal{L}_{BSM}$ contains only fields representing particles of spin ≤ 1.
4. the only fermion fields with chiral transformations under the gauge group G_{SM} are the ones of the SM. This means that all the extra fermions are vector-like with respect to G_{SM} (see next section for details).

In particular, assumption 2 is crucial for the perturbative unitarity of a theory which contains SM gauge bosons; the assumption 3 is to avoid renormalizability issues with interacting particles of spin > 1 [48]; the last requirement is due to the fact that a fourth generation of chiral fermions should couple to the Higgs doublet in order to gain mass, but this is excluded by observations.
Overall, these assumptions ensure that at low energies (where low means much smaller than the masses of the extra particles) the theory is well described by the SMEFT. This will turn out to be crucial in the following to be allowed to exploit all the model-independent results obtained within the effective theory framework.
In this work we are interested in the sector of $\mathcal{L}_{BSM}$ that can give contributions at the classical level to the dimension-six operators in SMEFT. It can be shown [49] that this can be realised by extra fields that can have gauge-invariant linear interactions with the SM fields of dimension $d \leq 4$. This condition strongly restricts the quantum number of the possible extra fields, which are collected in table 3.1, classified into irreducible representations of the Lorentz and gauge symmetry groups.
If all the vector bosons in the theory are the additional gauge bosons of an extended gauge symmetry $G \supset G_{SM}$ and $\mathcal{L}_{BSM}$ is invariant under G with no anomalies, then we obtain a unitary effective QFT that can be exploited to perform perturbative calculations to arbitrary precision at energies below the cutoff Λ. However, to keep a model-independent spirit, one should consider general theories without enforcing any gauge invariance beyond G_{SM}, so all the covariant derivatives appearing in the following are understood to be covariant only with respect to G_{SM}.
The part of the $\mathcal{L}_{BSM}$ that contributes classically to the effective Lagrangian of dimension $d \leq 6$ involves a finite number of fields and a finite number of operators. The complete Lagrangian can be

generally written as:

$$\mathcal{L}_{BSM} = \mathcal{L}_0 + \mathcal{L}_S + \mathcal{L}_F + \mathcal{L}_V + \mathcal{L}_{mix} + ... \tag{3.1}$$

where:

- $\mathcal{L}_0$ contains terms of $d \leq 6$ with only SM fields;
- $\mathcal{L}_{S,F,V}$ include terms of $d \leq 5$ with new scalars, fermions and vectors fields respectively, without products of new fields with different spin;
- $\mathcal{L}_{mix}$ contains terms of $d \leq 4$ with products of extra fields with different spin;
- the dots correspond to terms that do not contribute in our approximation.

In this thesis we choose to introduce new heavy fermions, as with respect to scalars their contributions to the effective operators $C_{u\phi}$, $C_{d\phi}$ turn out to carry less suppression factors (see [49], equations $D.61$, $D.63$).
In the following section, we will only present the relevant term for this work, namely $\mathcal{L}_F$, but each piece appearing in (3.1) can be found explicitely written in [49].

Scalar bosons								
Name	S	S_1	S_2	ϕ	Ξ	Ξ_1	Θ_1	Θ_3
Irrepr	$(1,1)_0$	$(1,1)_1$	$(1,1)_2$	$(1,2)_{1/2}$	$(1,3)_0$	$(1,3)_1$	$(1,4)_{1/2}$	$(1,4)_{3/2}$
Name	ω_1	ω_2	ω_4	Π_1	Π_7	ζ		
Irrepr	$(3,1)_{-1/3}$	$(3,1)_{2/3}$	$(3,2)_{-4/3}$	$(3,2)_{1/6}$	$(3,2)_{7/6}$	$(3,3)_{-1/3}$		
Name	Ω_1	Ω_2	Ω_4	Υ	Φ			
Irrepr	$(6,1)_{1/3}$	$(6,1)_{-2/3}$	$(6,1)_{4/3}$	$(6,3)_{1/3}$	$(8,2)_{1/2}$			
Vector-like fermions								
Name	N	E	Δ_1	Δ_3	Σ	Σ_1		
Irrepr	$(1,1)_0$	$(1,1)_{-1}$	$(1,2)_{-1/2}$	$(1,2)_{-3/2}$	$(1,3)_0$	$(1,3)_{-1}$		
Name	U	D	Q_1	Q_5	Q_7	T_1	T_2	
Irrepr	$(3,1)_{2/3}$	$(3,1)_{-1/3}$	$(3,2)_{1/6}$	$(3,2)_{-5/6}$	$(3,2)_{7/6}$	$(3,3)_{-1/3}$	$(3,3)_{2/3}$	
Vector bosons								
Name	$\mathcal{B}$	$\mathcal{B}_1$	$\mathcal{W}$	$\mathcal{W}_1$	$\mathcal{G}$	$\mathcal{G}_1$	$\mathcal{H}$	$\mathcal{L}_1$
Irrepr	$(1,1)_0$	$(1,1)_1$	$(1,3)_0$	$(1,3)_1$	$(8,1)_0$	$(8,1)_1$	$(8,3)_0$	$(1,2)_{1/2}$
Name	$\mathcal{L}_3$	$\mathcal{U}_2$	$\mathcal{U}_5$	$\mathcal{Q}_1$	$\mathcal{Q}_5$	$\mathcal{X}$	$\mathcal{Y}_1$	$\mathcal{Y}_5$
Irrepr	$(1,2)_{-3/2}$	$(3,1)_{2/3}$	$(3,1)_{5/3}$	$(3,2)_{1/6}$	$(3,2)_{-5/6}$	$(3,3)_{2/3}$	$(\bar{6},2)_{1/6}$	$(\bar{6},2)_{-5/6}$

Table 3.1: New scalar bosons, vector-like fermions and vector bosons contributing to the dimension-six SMEFT at tree level. The notation for the irreducible representation is: $(SU(3)_c, SU(2)_L)_Y$.

3.1 Our choice: Vector-like quarks

3.1.1 Why vector-like quarks?

Vector-like quarks are hypothetical spin 1/2 particles that transform as triplets under the colour gauge group and whose left- and right-handed components transform in the same way under the $SU(2)_L$ gauge group. This new kind of particles is very promising for several reasons. First of all, they are the simplest example of coloured fermions still allowed by experimental data. Indeed, extra quarks with chiral couplings, such as fourth generation quarks, are now excluded [50] by the recent measurements of Higgs-mediated cross sections [51, 52], when combined with direct searches at the Large Hadron Collider (LHC) [53, 54]. Vector-like quarks, on the other hand, do not need to receive their masses solely from Yukawa couplings to a Higgs doublet, since their explicit mass terms do not violate the gauge invariance, so they are consistent with existing Higgs data.
Secondly, they can mix with the SM quarks and thereby modify their couplings to the Z, W and Higgs boson. Thus, as we will discuss later, the addition of vector-like quarks to the SM implies

the modification of some observable quantities. For instance, they can give rise to tree-level flavour-changing neutral currents [55, 56] and they can introduce new sources of CP violation [57, 58].
Overall, the heavy VLQ at the TeV scale are well motivated scenarios, which have rich phenomenological implications and constitute a promising research field and appear in various context:

- as a solution to the hierarchy problem [59];
- to solve naturalness issues in supersymmetry [60];
- in little Higgs models [61];
- in models with partial compositeness (e.g. [62]).

All these reasons make VLQs an interesting possibility worthy of being explored. This motivates the choice of VLQ for our toy model.

3.1.2 Our selection of VLQ

The general Lagrangian $\mathcal{L}_F$ of (3.1) is given by:

$$\mathcal{L}_F = \mathcal{L}_F^{quad} + \mathcal{L}_F^{int}, \tag{3.2}$$

where

$$\mathcal{L}_F^{quad} = \sum_{\psi} \left[\bar{\psi} i \not{D} \psi - M_\psi \bar{\psi}\psi\right], \tag{3.3}$$

$$\mathcal{L}_F^{int} = \mathcal{L}^{(4)}_{leptons} + \mathcal{L}^{(4)}_{quarks} + \mathcal{L}^{(5)}_{leptons} + \mathcal{L}^{(5)}_{quarks}. \tag{3.4}$$

In our case, we are interested in the quark term of dimension 4.
The effective operators in (2.4) can be generated by heavy VL fermions, for instance as depicted in figure 3.1.

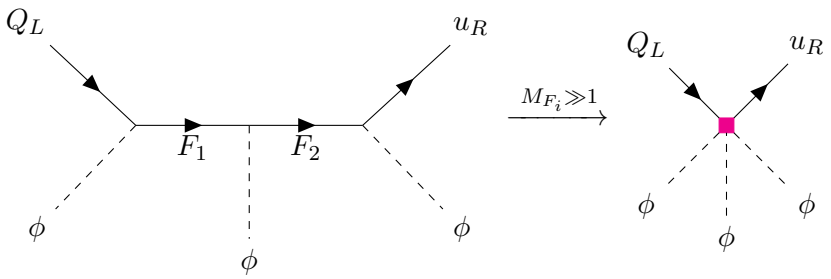

Figure 3.1: The effective operator $Q_{u\phi}$ can be generated at tree-level in the underlying heavy theory involving exchange of heavy VL fermions F_1, F_2 as depicted in the diagram on the left.

As anticipated in the last section, we need to include colored charged fermions, which means quarks, to ensure gauge invariance under $SU(3)_c$. Secondly, to respect $SU(2)_L$ invariance two types of $SU(2)_L$ VLQ multiplets could be adopted: (F_1, F_2) = (doublet, singlet) or (F_1, F_2) = (doublet, triplet). Finally, we have some freedom in choosing the hypercharge. The possible combinations of VLQ comparing in table 3.1 which could be adopted are reported in table 3.2.

	(doublet, singlet)	(doublet, triplet)
up	(Q_1, U), (Q_7, U)	(Q_1, T_1), (Q_1, T_2), (Q_7, T_2)
down	(Q_1, D), (Q_5, D)	(Q_1, T_1), (Q_1, T_2), (Q_5, T_2)

Table 3.2: VLQs possible combinations for the realization of figure 3.1, in the up and down sectors.

The simplest choice for each sector is the first option, namely:

- $SU(2)$ doublet $Q_{1i} = (Q_{1u}, Q_{1d})_i$

- up-type $SU(2)$ singlet U_i
- down-type $SU(2)$ singlet D_i

They correspond to the three VLQ located in table 3.3 with their quantum numbers. As one can observe, we are substantially adding three new particles which have the same quantum numbers of the SM quarks, but are vector-like and kave much heavier mass. Indeed, it is reasonable to assume a mass of few TeV in order to avoid the experimental constraints, especially electroweak precision tests. The mass of the VLQs defines the energy scale at which our UV model is working. In what follows, we will call this energy scale Λ and constrain it in chapter 5.
To mimic the SM situation and to construct a more general model, notice that we assume that U_i, D_i, Q_{1i} are each coming in three generations (i.e. $i = 1, 2, 3$).

Vector-like fermions			
Name	U_i	D_i	Q_{1i}
Irrepr	$(3,1)_{2/3}$	$(3,1)_{-1/3}$	$(3,2)_{1/6}$

Table 3.3: VLQ selection for the UV model. The notation for the irreducible representation is: $(SU(3)_c, SU(2)_L)_Y$.

To include these extra fields we need to introduce new terms to the SM Lagrangian:

$$-\mathcal{L}^{(4)}_{quarks} = (\lambda_U)_{ri}\bar{U}_{Rr}\tilde{\phi}^\dagger Q_{Li} + (\lambda_D)_{ri}\bar{D}_{Rr}\phi^\dagger Q_{Li} + (\lambda^u_{Q_1})_{ri}\bar{Q}_{1Lr}\tilde{\phi}u_{Ri} \tag{3.5}$$

$$+ (\lambda^d_{Q_1})_{ri}\bar{Q}_{1Lr}\phi d_{Ri} + (\lambda_{UQ_1})_{ri}\bar{U}_{Lr}\tilde{\phi}^\dagger Q_{1Ri} + (\lambda_{DQ_1})_{ri}\bar{D}_{Lr}\phi^\dagger Q_{1Ri} + \text{h.c.} \tag{3.6}$$

Notice the appearance of some free parameters of the new theory, in particular:

- The VLQ masses: $M_{U_i}, M_{D_i}$and $M_{Q_{1i}}$;
- The couplings of the VLQs to the SM particles: $\lambda_U, \lambda_D, \lambda^u_{Q_1}, \lambda^d_{Q_1}$;
- The couplings between VLQs: $\lambda_{UQ_1}, \lambda_{DQ_1}$.

The couplings λ are generic 3×3 matrices which in general implies flavor mixing. At this point, one could be interested in calculate explicitly, in the UV theory, how the new interaction terms can affect the interactions between the SM particles. Before performing the calculations, we need to pass to the mass basis in order for the propagators to be defined properly.
The complete Lagrangian is:

$$-\mathcal{L}_{down} = (\lambda_D)_{ri}\bar{D}_{Rr}\phi^\dagger Q_{Li} + (\lambda^d_{Q_1})_{ri}\bar{Q}_{1Lr}\phi d_{Ri} + (\lambda_{DQ_1})_{ri}\bar{D}_{Lr}\phi^\dagger Q_{1Ri} + y_d\bar{d}_R\phi^\dagger Q_L + \tag{3.7}$$

$$+ M_D\bar{D}_L D_R + M_{Q_1}\bar{Q}_{1L}Q_{1R} + \text{h.c.} \tag{3.8}$$

We pass to the unitary gauge:

$$-\mathcal{L}_{down}|_{u.g.} = \frac{v+h}{\sqrt{2}}\left[\lambda_D\bar{D}_R d_L + \lambda^d_{Q_1}\bar{Q}_{1dL}d_R + \lambda_{DQ_1}\bar{D}_L Q_{1dR} + y_d\bar{d}_R d_L\right] + M_D\bar{D}_L D_R + M_{Q_1}\bar{Q}_{1L}Q_{1R} + \text{h.c.} \tag{3.9}$$

Let us collect in matrix form the mass terms and the Higgs interactions:

$$-\mathcal{L}_{down}|_{u.g.} = \overline{\begin{pmatrix} d \\ D \\ Q_{1d} \end{pmatrix}}_R \underbrace{\begin{pmatrix} \frac{y_d v}{\sqrt{2}} & 0 & \frac{\lambda^d_{Q_1} v}{\sqrt{2}} \\ \frac{\lambda_D v}{\sqrt{2}} & M_D & 0 \\ 0 & \frac{\lambda^*_{DQ_1} v}{\sqrt{2}} & M_{Q_1} \end{pmatrix}}_{M} \begin{pmatrix} d \\ D \\ Q_{1d} \end{pmatrix}_L + \tag{3.10}$$

$$+ \overline{\begin{pmatrix} d \\ D \\ Q_{1d} \end{pmatrix}}_R \underbrace{\begin{pmatrix} \frac{y_d}{\sqrt{2}} & 0 & \frac{\lambda^d_{Q_1}}{\sqrt{2}} \\ \frac{\lambda_D}{\sqrt{2}} & 0 & 0 \\ 0 & \frac{\lambda^*_{DQ_1}}{\sqrt{2}} & 0 \end{pmatrix}}_{H} \begin{pmatrix} d \\ D \\ Q_{1d} \end{pmatrix}_L h + \text{h.c.} \tag{3.11}$$

Since d, D and Q_1 come in three generations, the matrices M and H are 9×9 generic matrices in flavor space. To pass to the mass basis, the matrix M has to be diagonalized through a biunitary transformation

$$V_d^\dagger M U_d = X, \qquad \text{with } X \text{ diagonal.} \tag{3.12}$$

The rotation matrices V_d and U_d are the ones that diagonalize the Hermitian matrices $M^\dagger M$ and $M M^\dagger$ respectively, namely:

$$\begin{cases} U_d (XX) U_d^\dagger = M^\dagger M \\ V_d (XX) V_d^\dagger = M M^\dagger \end{cases}, \qquad \text{with } XX = D^2 \text{ diagonal.} \tag{3.13}$$

In our case an exact analytical way to express the rotation matrices V_d and U_d was not found; the mass matrix can be diagonalized numerically using the `Mathematica` code with the singular value decomposition function.
However, we prefer to exploit the potency of the SMEFT: as we will see in the next chapter, this approach allows to perform all the required analysis in a model-independent fashion and match on the UV model only at the end.

Chapter 4

Matching and Running

After introducing the UV model and the SMEFT framework, the next step is to establish a connection between the two. As anticipated, the strategy is to use SMEFT as a bridge to connect our UV model to the precision observables and constrain the UV parameters. This connection is established through a three-step procedure, which is schematically illustrated in the figure 4.1:

1. Match the UV model onto the SMEFT at high scale Λ. This provides the Wilson coefficients as a function of the UV parameters at the scale Λ.
2. Run the Wilson coefficients down to the weak scale, using the renormalization group equations (RGE) of the SMEFT [63–66].
3. Map the Wilson coefficients onto observables, for instance compute the weak scale observables using the effective Lagrangian at the weak scale.

In this chapter we discuss step 1 and step 2, while we leave the last step for the next chapter.

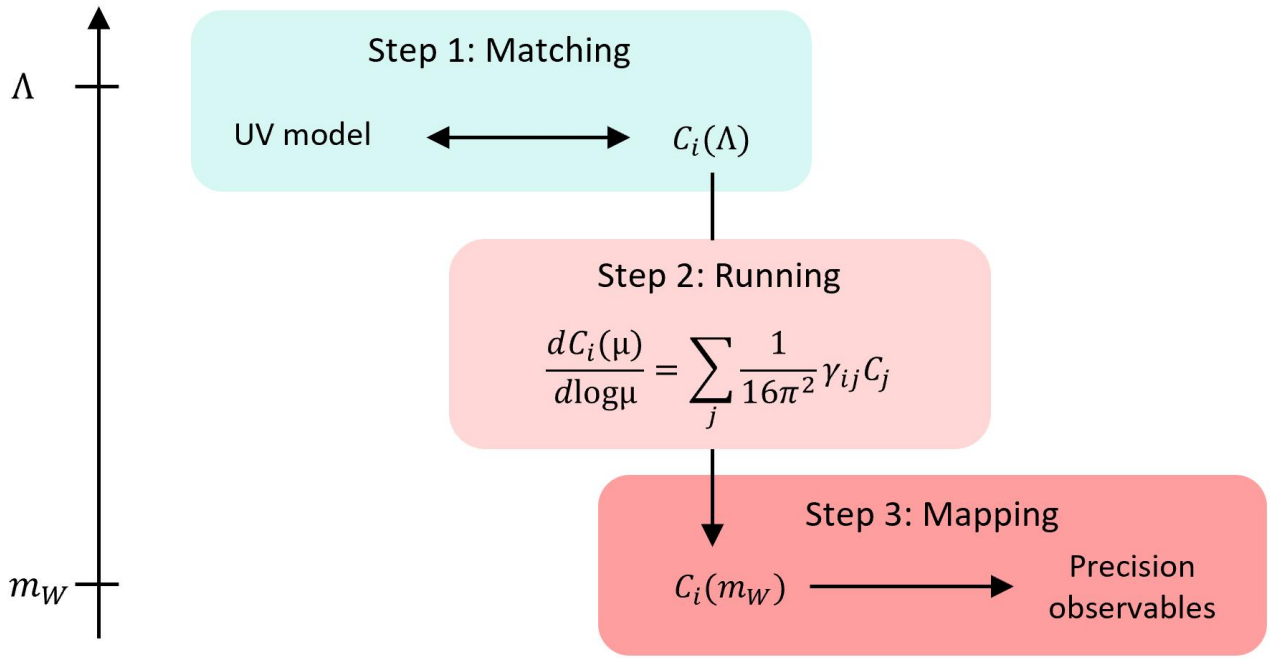

Figure 4.1: The connection scheme between UV models and weak scale precision observables using SMEFT as a bridge.

4.1 UV theory and EFT Matching

In order to study the physics of $\mathcal{L}_{BSM}$ at energy scales much below the masses of the extra particles, we can use an effective Lagrangian. Via matching a correspondence between the EFT parameters and the UV parameters is obtained by calculating S matrix elements both in the EFT and the UV completion. The results are then equated at a fixed energy scale. This defines the matching conditions that fixes the Wilson coefficients in terms of the parameters of the UV completion.

To obtain the low energy limit of the UV calculations, the heavy fields are integrated out. This approach was developed by Wilson [67, 68] and at the classical level can be performed by

1. eliminating the heavy fields by using the equation of motion of $\mathcal{L}_{BSM}$;
2. expanding the propagators of the heavy fields in inverse powers of D/M, where D and M stand for covariant derivative and heavy particle mass, respectively.

At any finite order in D/M the result of the procedure is a local Lagrangian. This is the so called functional approach. Equivalently, the first step can be completed in terms of Feynman diagrams, which in many cases it's an easier path.
Let us consider for instance the effective operator

$$Q_{d\phi} = (\phi^\dagger \phi)(\bar{Q}_L \phi d_R). \tag{4.1}$$

It generates the following Feynman diagram, whose correspondent Feynman amplitude $\mathcal{M}$ is given by

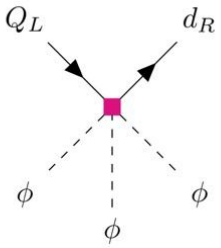

$$\mathcal{M} = i(C^\dagger_{d\phi})^{ij} \bar{u}_{d^j_R}(p') u_{Q^i_L}(p)$$

On the other hand, this effective operator can be generated in the underlying NP theory by the mediation of the heavy VLQ D and Q_1 as follows

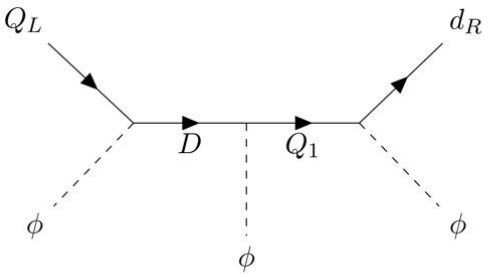

$$\mathcal{M} = i(\lambda^d_Q)^*_{jr} i(\lambda_{DQ_1})^*_{sr} i(\lambda_D)_{si} \bar{u}_{d^j_R}(p') \Delta_{Q^r_1}(p_2) \Delta_{D^s}(p_1) u_{Q^i_L}(p).$$

where the Feynman rules of the vertices can be derived by (3.7) and the fermionic propagator is

$$\Delta(p_i) = -\frac{i\not{p}_i + M}{M^2}\left(1 - \frac{p_i^2}{M^2}\right) + \mathcal{O}(1/M^5). \tag{4.2}$$

In the low energy limit, i.e. assuming that the external momentum is much smaller than the VLQ masses, the propagators reduce to $\Delta = -1/M$, thus equating the two amplitudes gives:

$$(C_{d\phi})_{ij}|_{D,Q_1} = -\frac{(\lambda_{DQ_1})_{sr}(\lambda_D)^*_{si}(\lambda^d_{Q_1})_{rj}}{M_{Q_{1r}} M_{D_s}} \tag{4.3}$$

The Wilson operator $Q_{d\phi}$ receives also contributions from diagrams which involve only one type of extra particles, namely [49]:

$$(C_{d\phi})_{ij}|_{1\text{ type}} = \frac{y^{d*}_{jk}(\lambda_D)_{rk}(\lambda_D)^*_{ri}}{2M^2_{D_r}} + \frac{y^{d*}_{ki}(\lambda^d_{Q_1})_{rj}(\lambda^d_{Q_1})^*_{rk}}{2M^2_{Q_{1r}}} + ... \tag{4.4}$$

These contributions clearly suffer from a further suppression with respect to contribution (4.3) given by the Yukawa factor. For this reason, we decide to neglect these contributions and to focus on the one in (4.3).

The extra fields we chose to introduce in our BSM theory appearing in table 3.3 generate the effective operators shown in table 4.1 [49] and defined in table 2.1.

Fields	Operators
U	$Q_{u\phi},\ Q^{(1)}_{\phi q},\ Q^{(3)}_{\phi q}$
D	$Q_{d\phi},\ Q^{(1)}_{\phi q},\ Q^{(3)}_{\phi q}$
Q_1	$Q_{u\phi},\ Q_{d\phi},\ Q_{\phi u},\ Q_{\phi d},\ Q_{\phi ud}$

Table 4.1: Operators generated by the heavy VLQs in table 3.3.

All the tree-level contributions to the Wilson coefficients of the dimension-six SMEFT in UV completions with general extra particles can be found in literature, for example in [49].
We report here the matching of the operators of interest. Two kinds of indices appears: $r, s = 1, 2, 3$ indicate the VLQs generations, while $i, j = 1, 2, 3$ indicate the SM-quarks generations.

$$(C_{d\phi})_{ij}|_{D,Q_1} = -\frac{(\lambda_{DQ_1})_{sr}(\lambda_D)^*_{si}(\lambda^d_{Q_1})_{rj}}{M_{Q_{1r}}M_{D_s}}, \qquad (C_{\phi d})_{ij}|_{Q_1} = \frac{(\lambda^d_{Q_1})_{rj}(\lambda^d_{Q_1})^*_{ri}}{2M^2_{Q_{1r}}}, \tag{4.5}$$

$$(C_{u\phi})_{ij}|_{U,Q_1} = -\frac{(\lambda_{UQ_1})_{sr}(\lambda_U)^*_{si}(\lambda^u_{Q_1})_{rj}}{M_{Q_{1r}}M_{U_s}}, \qquad (C_{\phi u})_{ij}|_{Q_1} = \frac{(\lambda^u_{Q_1})_{rj}(\lambda^u_{Q_1})^*_{ri}}{2M^2_{Q_{1r}}}, \tag{4.6}$$

$$(C^{(1)}_{\phi q})_{ij}|_{D,U} = \frac{(\lambda_U)_{rj}(\lambda_U)^*_{ri}}{4M^2_{U_r}} - \frac{(\lambda_D)_{rj}(\lambda_D)^*_{ri}}{4M^2_{D_r}}, \qquad (C_{\phi ud})_{ij}|_{Q_1} = \frac{(\lambda^d_{Q_1})_{rj}(\lambda^u_{Q_1})^*_{ri}}{2M^2_{Q_{1r}}}, \tag{4.7}$$

$$(C^{(3)}_{\phi q})_{ij}|_{D,U} = -\frac{(\lambda_U)_{rj}(\lambda_U)^*_{ri}}{4M^2_{U_r}} - \frac{(\lambda_D)_{rj}(\lambda_D)^*_{ri}}{4M^2_{D_r}}. \tag{4.8}$$

Notice that we changed notation with respect to chapter 2: here and in the following, the Wilson coefficients have mass dimension -2, namely the factor $1/\Lambda^2$ is inglobated in C_i. This has to be kept in mind, and we hope it will not be source of confusion when in chapter 5 the masses of the VLQs will be set to Λ to obtain constraints on the NP energy scale.

4.2 Running

To connect with measurements, the Wilson coefficients $C_i(\Lambda)$ in (4.3) need to be evolved from the matching scale Λ down to the weak scale μ_{EW}, according to their renormalization group (RG) equation. The concept of RG arises from comparing physical quantities at different length/energy scales. Let us consider a physical quantity $\mathcal{A}(g_i; E)$ which can depend in general on a set of couplings g_i and an energy scale E. Being an artificial parameter, if the cut-off of the theory μ is changed, physics on energies scales below μ has to remain constant, so the RG theory postulates that the couplings must change with μ. The RG flow of the theory is determined by imposing that

$$\mathcal{A}(g_i(\mu); E)_\mu = \mathcal{A}(g_i(\mu'); E)_{\mu'}. \tag{4.9}$$

The dependence of a coupling g(μ) on the energy-scale is known as "running of the coupling".
As anticipated in figure 4.1, the RG equations that relate the Wilson coefficients at different scales at

leading order are governed by the anomalous dimension of the operator basis γ_{ij}:

$$\frac{dC_i(\mu)}{d\log\mu} = \sum_j \frac{1}{16\pi^2}\gamma_{ij}C_j. \tag{4.10}$$

The anomalous dimension matrix encodes operator mixing effects and its computation is a non trivial task. Fortunately, RG running is intrinsic to the SMEFT and hence only need to be done once even for different UV model. In recent years, there has been significant exploration into the RG evolution of the SMEFT. In particular, great progress has been made in the determination of the anomalous dimension matrix γ_{ij}: remarkably, the entire one-loop anomalous dimension matrix within a complete operator basis is available in literature [63–66].
The RG analysis is a conceptually important step and it can provide relevant corrections to the SM amplitudes: in particular, the SM parameters have anomalous dimension contributions of order v^2/Λ^2 from coefficients in the dimension-six Lagrangian, which lead to corrections of the same order of the ones coming from dimension-six operators [63].
To understand when the running of Wilson coefficients is of practical relevance, one needs to remind that the estimated sensitivity of near future measurements is at the per mille level, so perturbative calculation can be truncated at one loop.
Since RG evolution contributes as a loop factor, the general rule of thumb is that the RG evolution of $C_i(\Lambda)$ is relevant for into $C_j(\mu_{EW})$ when $C_i(\Lambda)$ is generated at tree level from the UV model (because otherwise its contribution would be of higher order loop size) and $C_j(\Lambda)$ is not generated at tree level (because in this case the contribution of into $C_i(\Lambda)$ is subdominant).
For instance, our selection of VLQ generates at tree level the operator $Q^{(1)}_{\phi q}$ but not the operator $Q^{(1)}_{qq}$ (which is relevant e.g. for flavor changing neutral currents processes). Then, operators mixing, namely the introduction of $C^{(1)}_{qq}(\mu_{EW})$ by the RGE running from $C^{(1)}_{\phi q}(\Lambda)$ can turn out to set relevant constraints.
In order to illustrate the assumptions we use when performing the RGE, let us consider the running of $C^{(1)}_{qq}$ that can be found in appendix A.8 of [64]:

$$\dot{C}^{(1)}_{qq} = \frac{1}{2}\left[Y_u^\dagger Y_u - Y_d^\dagger Y_d\right]C^{(1)}_{\phi q} \qquad \text{where } \dot{C} \equiv 16\pi^2\mu\frac{d}{d\mu}C \tag{4.11}$$

The term in squared brackets is the anomalous dimension written in terms of the Yukawa matrices.
In first approximation, the RGE analysis can be simplified assuming the so-called leading log (LL) approximation, which consists in considering the right hand side independent from the running scale μ.
Within this approximation, the equation (4.11) becomes a differential equation which can be solved by separating variables. The result is:

$$C^{(1)}_{qq}|_{LL} = \frac{1}{64\pi^2}\left[Y_u^\dagger Y_u - Y_d^\dagger Y_d\right]C^{(1)}_{\phi q} \cdot \log\left(\frac{\mu^2}{\Lambda^2}\right). \tag{4.12}$$

In general, the LL approximation leads to

$$\mu\frac{d}{d\mu}C_i = \sum_j \frac{1}{16\pi^2}\gamma_{ij}C_j \qquad \xrightarrow[LL]{} \qquad C_i(\mu) = C_i(\Lambda) + \frac{1}{16\pi^2}\log\left(\frac{\mu}{\Lambda}\right)\sum_j \gamma_{ij}C_j(\Lambda). \tag{4.13}$$

Chapter 5

Experimental limits

The final step is to check that all the observables that receive a modification of our NP scenario remain within their experimental bounds. In the past decade, indeed, the scientific community has accumulated a wealth of very precise measurements worldwide, which substantially confirm the validity of the SM with astonishing precision. For our interests, the most stringent bounds come from flavour physics, from electroweak precision tests and Higgs physics.
In the following sections each of them will be considered in detail, but we can anticipate that they share the same procedure: the Wilson coefficients are run down to the energy scale of the experimental bounds and mapped onto the observables. Subsequently, the constraints on the Wilson coefficients are translated to constraints on the UV model.
We found that the most effective way to tune our UV parameters is to fix the values of the couplings and to obtain the constraint on Λ. The final results will be discussed in the last chapter, but from preliminary estimates we suggest to keep in mind that $\Lambda \sim 5$ TeV is sufficient to obtain a two-orders-of-magnitude enhancement of the light quark Yukawa couplings.

5.1 Flavour Changing Neutral Currents

The first experimental bounds which can constrain our UV model regard flavour physics. In particular, the flavour changing neutral current processes (FCNC) are processes with a change of flavor without a net charge transfer of fermions. Remarkable examples of FCNC are meson decays like $K_L \to \mu^+\mu^-$ and meson-antimeson oscillations like $K^0 - \bar{K}^0$.

As seen in the first section, in the SM flavor changing processes are mediated only by the charged current (CC) sector of the SM Lagrangian at tree level. An example can be found in figure 5.1.

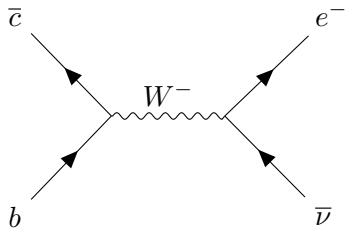

Figure 5.1: Example of flavour changing charged current (FCCC).

On the contrary, the Z-bosons and photons couple up to up and down to down, so they remain diagonal in the mass basis. This implies that in the SM FCNC are not allowed at tree level.
However, they can arise at loop level through the mediation of CC interactions, for instance as shown in figure 5.2.

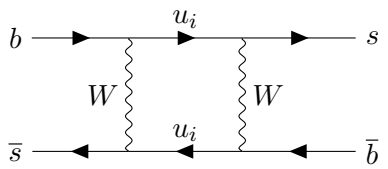

Figure 5.2: Example of meson-antimeson oscillation, particularly the $B_s^0 = (\bar{b}s) \longleftrightarrow \bar{B}_s^0 = (b\bar{s})$.

Beside being loop suppressed, in the SM meson-antimeson oscillations suffer from further suppression via the Glashow-Iliopoulos-Maiani (GIM) mechanism [69]. Introduced in 1970 to explain the suppression of the $\Delta S = 2$ processes, the GIM mechanism predicted the existence of a fourth quark, the charm. Relying on the unitarity of the charged weak current flavor, the FCNC box diagrams are suppressed by the mass difference between the various virtual quarks. The most relevant oscillations of the neutral pseudoscalar mesons M^0 in their antiparticle $\bar{M}^0$ are:

- Kaons: $K^0 = (\bar{s}d) \longleftrightarrow \bar{K}^0 = (s\bar{d})$;
- D mesons: $D^0 = (\bar{u}c) \longleftrightarrow \bar{D}^0 = (u\bar{c})$;
- B mesons: $B_d^0 = (\bar{b}d) \longleftrightarrow \bar{B}_d^0 = (b\bar{d})$ and $B_s^0 = (\bar{b}s) \longleftrightarrow \bar{B}_s^0 = (b\bar{s})$.

The oscillation phenomenon implies that M and $\bar{M}$, with $M = K^0, D^0, B_d^0, B_s^0$, are not mass eigenstates. The flavor basis consists of

$$|M^0\rangle = \begin{pmatrix} 1 \\ 0 \end{pmatrix} \qquad \text{and} \qquad |\bar{M}^0\rangle = \begin{pmatrix} 0 \\ 1 \end{pmatrix}. \tag{5.1}$$

The meson-antimeson system is described by an Hamiltonian made of two pieces: a mixing matrix M and a decay matrix Γ

$$H = M - \frac{i}{2}\Gamma. \tag{5.2}$$

The mixing matrix and the decay matrix are 2×2 hermitian matrices in the flavour basis. By exploiting CPT invariance and the hermitianity of the matrices M, Γ we can write the Hamiltonian in the matricial form

$$H = \begin{pmatrix} M_{11} - \frac{i}{2}\Gamma_{11} & M_{12} - \frac{i}{2}\Gamma_{12} \\ M_{21} - \frac{i}{2}\Gamma_{21} & M_{22} - \frac{i}{2}\Gamma_{22} \end{pmatrix} = \begin{pmatrix} M - \frac{i}{2}\Gamma & M_{12} - \frac{i}{2}\Gamma_{12} \\ M_{12}^* - \frac{i}{2}\Gamma_{12}^* & M - \frac{i}{2}\Gamma \end{pmatrix}. \tag{5.3}$$

Particularly, the M_{12} element encodes the mixing probability. When diagonalizing the Hamiltonian, two eigenvalues are found. Using the common notation (L for light, H for heavy) we find

$$\mu_{L,H} = (M - \frac{i}{2}\Gamma) \pm \sqrt{(M_{12} - \frac{i}{2}\Gamma_{12})(M_{12}^* - \frac{i}{2}\Gamma_{12}^*)} = m_{L,H} - \frac{i}{2}\Gamma_{L,H}. \tag{5.4}$$

Thus we define

$$\begin{cases} \Delta m = m_H - m_L, \\ \Delta\Gamma = \Gamma_L - \Gamma_H, \end{cases} \tag{5.5}$$

which are the measurable quantities.
The off-diagonal element of the mass matrix mixing can obtain contributions from NP as follows:

$$M_{12} = [M_{12}]_{\text{SM}} + [M_{12}]_{\text{BSM}}. \tag{5.6}$$

In meson-antimeson oscillations the flavour is violated by two units: for this reason, they are commonly known as $\Delta F = 2$ processes. The effects from $\Delta F = 1$ processes are expected to be subdominant with respect to the $\Delta F = 2$ case and will be neglected in this work. In some scenarios $\Delta F = 1$ transitions can though give dominant bounds if $\Delta F = 2$ suffer from suppression.

5.1.1 $\Delta F = 2$ from NP

The most important Wilson coefficients of SMEFT operators that contribute to $\Delta F = 2$ processes are

$$\{Q_{qq}^{(1)}, Q_{qq}^{(3)}, Q_{qa}^{(1)}, Q_{qa}^{(8)}, Q_{aa}\}, \tag{5.7}$$

where a stands for u, d. As shown in table 4.1, our UV model does not generate any of operators in (5.7) at tree level . However, they arise through their RG evolution, receiving contributions from operators

$$\{Q_{\phi q}^{(1)}, Q_{\phi q}^{(3)}, Q_{\phi u}, Q_{\phi d}, Q_{\phi ud}\}. \tag{5.8}$$

The observables related to meson-antimeson oscillations are measured at energy scales $\mu = \mu_{\text{had}}$ of few GeV, which is set by the masses of the neutral mesons. For this reason, it is convenient to parameterize the contributions from NP within the Low Effective Field Theory (LEFT), which is the effective field theory obtained from the SM by the decoupling of the heavy electroweak gauge bosons, the Higgs field and the top quark. The effective Hamiltonian [70] of interest for $\Delta F = 2$ processes can be written as:

$$\mathcal{H}_{\Delta F=2}^{ij} = [\mathcal{H}_{\Delta F=2}^{ij}]_{SM} + \sum_a C_a^{ij}(\mu) Q_a^{ij}, \tag{5.9}$$

where $ij = ds$ for kaon mixing and $ij = sb, db$ for B-mesons mixing. The SM term consists in only one $\Delta F = 2$ operator

$$Q_{VLL}^{ij} = [\bar{d}_i \gamma_\mu P_L d_j][\bar{d}_i \gamma^\mu P_L d_j]. \tag{5.10}$$

The $\Delta F = 2$ effective operators Q_a^{ij} appearing in the second term with their respective Wilson coefficients C_a^{ij} parameterize the BSM contributions to observables. In particular, in the case of the off-diagonal element of the mass matrix one has [71]

$$[M_{12}^{ij}]_{\text{BSM}} = \frac{1}{2M_{M^0}} \sum_a C_a^{ij}(\mu) \langle Q_a^{ij}(\mu) \rangle + \mathcal{O}(\text{dim-8}), \tag{5.11}$$

where the hadronic matrix elements of the operators

$$\langle Q_a^{ij}(\mu) \rangle = \langle M^0 | Q_a^{ij}(\mu) | \bar{M}^0 \rangle \tag{5.12}$$

are calculated with non-perturbative methods like Lattice Quantum Chromodynamics (LQCD). In the past, several $\Delta F = 2$ operator bases have been chosen, for example the Buras-Misiak-Urban (BMU) basis [72], the SUSY basis [73] and the Jenkins-Manohar-Stoffer (JMS) basis [74]. The latter is particularly useful for the purpose of matching with SMEFT. Indeed, a full one-loop matching of SMEFT to LEFT in the JMS basis can be found in [75]. As illustrated in figure 5.3, the experimental constraints on UV models can be obtained following the procedure:

1. Match the UV theory and the SMEFT at the high scale Λ. This provides the Wilson SMEFT coefficients in terms of UV parameters ($C_b(\Lambda)$).
2. Run down the SMEFT coefficients to the electroweak scale. This includes RGE mixing of the SMEFT Wilson coefficients into $C_a(\mu_{EW})$.
3. Match the SMEFT and the LEFT at the scale μ_{EW}. This provides the Wilson coefficients of LEFT in terms of the ones of SMEFT at the weak scale ($C_i(\mu_{\text{EW}})$).
4. Run down the LEFT coefficients to the energy scale of measurements. This provides $C_j(\mu_{\text{had}})$.
5. Map the weak Wilson coefficients $C_j(\mu_{\text{had}})$ into observables.

5.1.2 Experimental bounds on our UV model

In order to put experimental bounds on our UV model, we used the constraints in [2]. This work provides the model-independent bounds on the SMEFT from flavor physics, derived by following the procedure illustrated in the previous section. In particular, these constraints are obtained from $K - \bar{K}$,

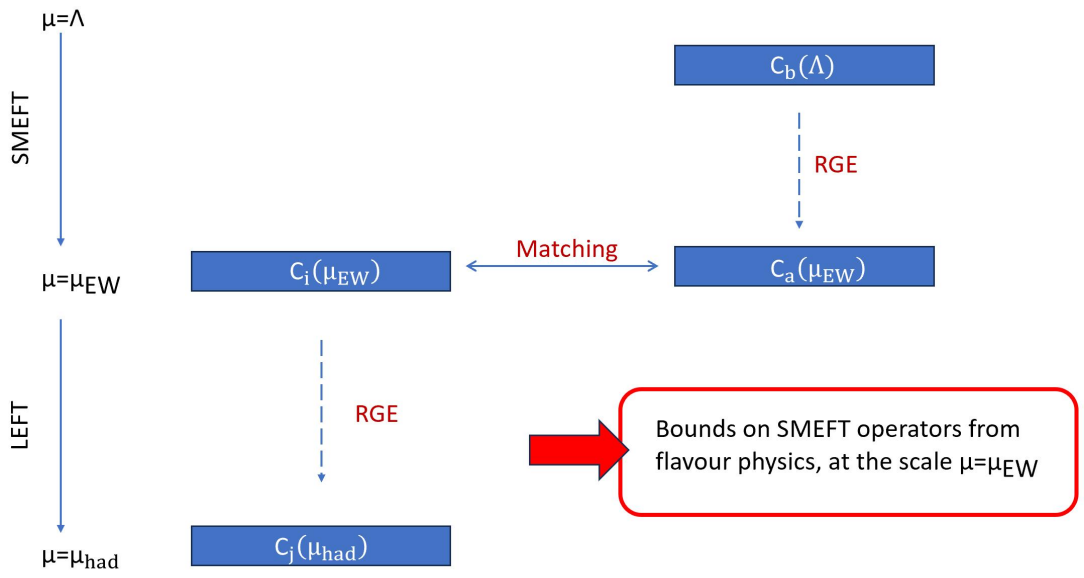

Figure 5.3: The connection scheme between UV models and low scale precision observables using SMEFT and LEFT as a bridge.

$D-\bar{D}$, $B_d-\bar{B}_d$ and $B_s-\bar{B}_s$ mixing and constrain the (real, imaginary) parts of Wilson coefficient of the $\Delta F=2$ weak Hamiltonian. These bounds are translated into bounds on Wilson coefficients of 5.7 and presented for the real and imaginary part of each element, at the scale $\Lambda=1$ TeV.

Thus, to study how the constraints on the SMEFT Wilson coefficients presented in [2] translate in turn into bounds on our UV parameters, we adhered to the following procedure:

1. Run down to the scale $\mu=1$TeV, which is the scale at which [2] gives their bounds, by solving the RGE for the operators (5.7) in the leading log approximation, and considering the mixing with the operators (5.8) that are generated at tree level (see figure 5.4).
2. Write the operators in terms of the UV parameters exploiting the matching expressions at the NP scale.
3. Consider, element by element, the bounds on $\{C_{qq}^{(1)}, C_{qq}^{(3)}, C_{qa}^{(1)}, C_{qa}^{(8)}, C_{aa}\}$ coming from [2].

In the first step we considered the RG running contribution of Yukawa matrices, given in [64], which assuming the LL approximation lead to the following equations:

$$(C_{qq}^{(1)})_{[prst]} = \frac{1}{64\pi^2}\left(\left[Y_u^\dagger Y_u - Y_d^\dagger Y_d\right]_{pr}(C_{\phi q}^{(1)})_{st}\cdot\log\left(\frac{\mu^2}{\Lambda^2}\right) + \left[Y_u^\dagger Y_u - Y_d^\dagger Y_d\right]_{st}(C_{\phi q}^{(1)})_{pr}\cdot\log\left(\frac{\mu^2}{\Lambda^2}\right)\right) \tag{5.13}$$

$$(C_{qq}^{(3)})_{[prst]} = -\frac{1}{64\pi^2}\left(\left[Y_u^\dagger Y_u + Y_d^\dagger Y_d\right]_{pr}(C_{\phi q}^{(1)})_{st}\cdot\log\left(\frac{\mu^2}{\Lambda^2}\right) + \left[Y_u^\dagger Y_u + Y_d^\dagger Y_d\right]_{st}(C_{\phi q}^{(1)})_{pr}\cdot\log\left(\frac{\mu^2}{\Lambda^2}\right)\right) \tag{5.14}$$

$$(C_{uu})_{[prst]} = -\frac{1}{32\pi^2}\left(\left[Y_u^\dagger Y_u\right]_{pr}(C_{\phi u})_{st}\cdot\log\left(\frac{\mu^2}{\Lambda^2}\right) + \left[Y_u^\dagger Y_u\right]_{st}(C_{\phi u})_{pr}\cdot\log\left(\frac{\mu^2}{\Lambda^2}\right)\right) \tag{5.15}$$

$$(C_{dd})_{[prst]} = \frac{1}{32\pi^2}\left(\left[Y_d^\dagger Y_d\right]_{pr}(C_{\phi d})_{st}\cdot\log\left(\frac{\mu^2}{\Lambda^2}\right) + \left[Y_d^\dagger Y_d\right]_{st}(C_{\phi d})_{pr}\cdot\log\left(\frac{\mu^2}{\Lambda^2}\right)\right) \tag{5.16}$$

$$(C_{qu}^{(1)})_{[prst]} = \frac{1}{32\pi^2}\left(\left[Y_u^\dagger Y_u - Y_d^\dagger Y_d\right]_{pr}(C_{\phi u})_{st}\cdot\log\left(\frac{\mu^2}{\Lambda^2}\right) - 2\left[Y_u Y_u^\dagger\right]_{st}(C_{\phi q}^{(1)})_{pr}\cdot\log\left(\frac{\mu^2}{\Lambda^2}\right)\right) \tag{5.17}$$

$$(C_{qd}^{(1)})_{[prst]} = \frac{1}{32\pi^2}\left(\left[Y_u^\dagger Y_u - Y_d^\dagger Y_d\right]_{pr}(C_{\phi d})_{st}\cdot\log\left(\frac{\mu^2}{\Lambda^2}\right) + 2\left[Y_d Y_d^\dagger\right]_{st}(C_{\phi q}^{(1)})_{pr}\cdot\log\left(\frac{\mu^2}{\Lambda^2}\right)\right) \tag{5.18}$$

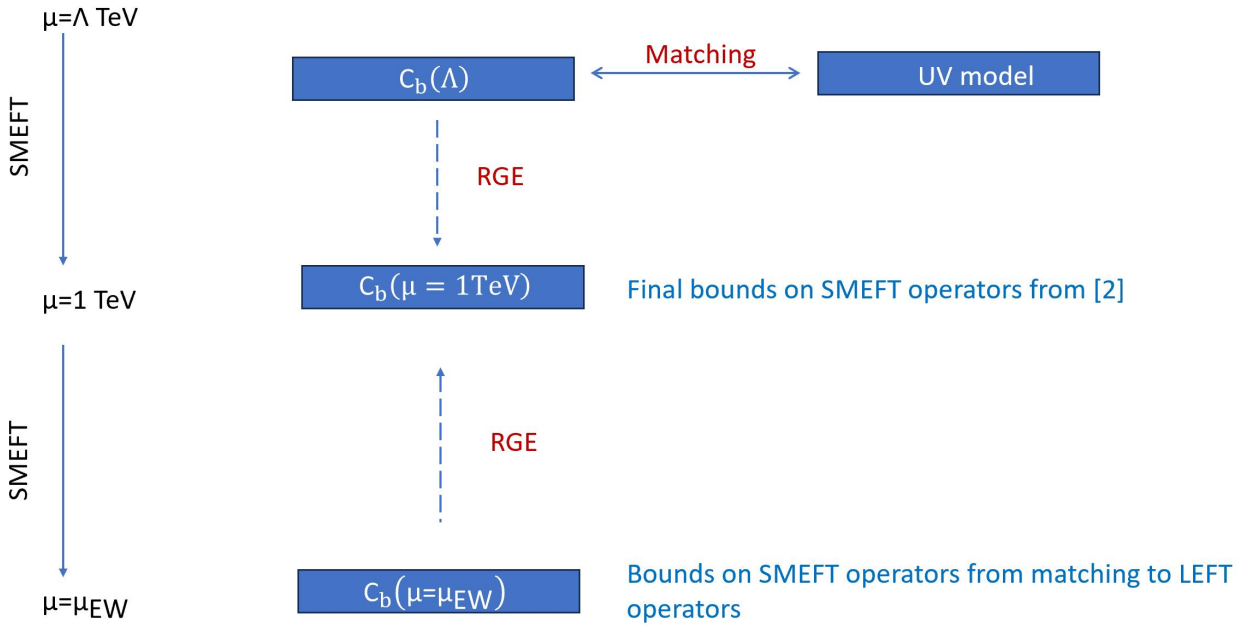

Figure 5.4: The energy scales scheme of the procedure.

At that point, we obtained a system of equations with the NP couplings λ_i and the masses of the VLQs as free parameters. To obtain analytic constraints using `Mathematica`, some assumptions were in need. First of all, the coupling matrices λ were assumed flavor diagonal and universal, namely

$$\lambda_\star^{ij} = \lambda_\star \begin{pmatrix} 1 & & \\ & 1 & \\ & & 1 \end{pmatrix} \qquad \text{with } \lambda_\star = \lambda_{U,D}, \lambda_{Q1}^{u,d}, \lambda_{UQ_1}, \lambda_{DQ_1}. \tag{5.19}$$

With this assumption, the contributions to the Wilson coefficients simplify a lot, leading to several cancellations in most of the elements. In particular, all the Wilson coefficients become diagonal, which implies that only the elements $[aaxy]$ or $[xyaa]$ are non-vanishing, with $x, y, a = 1, 2, 3$.
Secondly, in order to derive bounds from the ones presented in [2], the couplings were set to 1 and the masses of the VLQs were all set to Λ, allowing to obtain a constraint on Λ.
Using equations (5.14)-(5.18) one obtains

$$C_{[aaxy]}|_{\text{computed}} = \frac{b \cdot \log(\frac{1}{\Lambda^2})}{\Lambda^2} \tag{5.20}$$

where with Λ we indicated the NP scale expressed in TeV, and with b a numerical constant. Then we impose

$$C_{[aaxy]}|_{\text{computed}} \leq C_{[aaxy]}|_{\text{bound}}. \tag{5.21}$$

From this equation we get the minimum Λ to respect the flavor bounds setting the Wilson coefficient with natural values.
For simplification, we considered two cases in which either up-type or down-type VLQs are present, namely:

- $\lambda_D, \lambda_Q^d, \lambda_{DQ_1} = 1$ and $\lambda_U, \lambda_Q^u, \lambda_{UQ_1} = 0$;
- $\lambda_D, \lambda_Q^d, \lambda_{DQ_1} = 0$ and $\lambda_U, \lambda_Q^u, \lambda_{UQ_1} = 1$.

Relevant differences between the two cases were not found, so we will present the results just once.
In the case with both up-type and down-type VLQs, the only difference is in operators $Q_{\phi q}^{(1,3)}$, since the other operators in (5.8) depend on just one type of VLQ (see the matching relations in chapter 4).
The experimental bounds on $Q_{\phi q}^{(1,3)}$ can be trivially satisfied e.g. by choosing equal $\lambda_\star$.
We present in table 5.1 the bounds obtained from each Wilson coefficient, providing only the element

Operator	Element	Meson type	Bound on Λ (TeV)
$C_{qq}^{(1)}$	1122	$K-\bar{K}$	0.998
$C_{qq}^{(3)}$	1133	$K-\bar{K}$	0.959
$C_{qd}^{(1)}$	3311	$K-\bar{K}$	0.149
$C_{qu}^{(1)}$	1133	$K-\bar{K}$	0.617
C_{dd}	2223	$B_s-\bar{B}_s$	0.001

Table 5.1: Bounds on Λ from $\Delta F = 2$ constraints, up basis.

which implied the stringest bound. The most significant is the first one, i.e. the one coming from $C_{qq}^{(1)}$, which requires Λ of almost ~ 1 TeV.
An opposite analysis was also performed: the energy scale Λ was set to 2 TeV and all the couplings were set to λ. The upper limits obtained on λ were highly beyond perturbative values. For this reason we chose to show only the constraints on Λ.

5.2 Electroweak Precision Tests (EWPT)

One of the most constraining limits stem from Z-pole measurements at LEP, namely that set of experiments and measurements in particle physics designed to test the predictions of the electroweak theory. They concern physical observables which are only sensitive to the electroweak sector, for example

- the electron magnetic dipole moment g.
- the decay rate of the muon Γ_μ.
- the Z boson pole mass M_Z.
- the W boson pole mass M_W.
- the polarization asymmetry in the Z boson production A_{LR}.

These precision tests are crucial because they provide stringent constraints on the parameters of the electroweak theory and can reveal any deviations or inconsistencies with experimental data. The success of the electroweak theory in accurately predicting the outcomes of these tests has been a significant triumph of particle physics and has led to a deeper understanding of the fundamental forces and particles in the universe.
In addition to testing the SM, EWPT can also be used to perform model-independent analysis, to place constraints on new physics models.
Among the strongest bounds are those on operators that modify the vector-boson self-energies, which however are not generated by our UV model. From the current experimental limits on electric dipole moments (EDMs) and anomalous magnetic moments can constrain the dipole operators Q_{uW}, Q_{uB}, Q_{uG}, Q_{dW}, Q_{dB}, Q_{dG} [1, 76], but again we do not generate contributions to this operators.
On the contrary, we do have to consider the operators $C_{\phi q}^{(1)}$, $C_{\phi q}^{(3)}$, $C_{\phi u}$ and $C_{\phi d}$, which are strongly constrained by Z-pole measurements, as they modify the couplings to quarks. In the next paragraph, we explain how the results of [77] can be used to perform a fit on these Wilson coefficients and consequently obtain bounds.

5.2.1 Bounds from Z-pole observables

The bounds on dimension 6-operators coming from EWPT can be obtained as explained in [1]. In this work they construct a likelihood for a given observable O as follows:

$$L \propto \exp[-\frac{(O_{SM}+\delta O - O_{exp})^2}{2\Delta O_{exp}^2}], \tag{5.22}$$

where $O_{exp} \pm \Delta O_{exp}$ is the experimental value of the observable, O_{SM} is its SM prediction and δO is the correction due to the effective operators. A likelihood was constructed for the various coefficients by computing their contributions to the Z-pole observables. Two fits were performed separately: one on the coefficients of the operators involving the light quarks (u, d, s) and one on operators involving charged leptons and heavy quarks (c, b). The relevant observables for the first fit are

- the Z total width Γ_{tot},
- the hadronic pole cross section σ_{had}, defined as

$$\sigma_{had} = \frac{12\pi}{M_Z^2}\frac{\Gamma_{ee}\Gamma_{had}}{\Gamma_Z^2} \tag{5.23}$$

- the parameter R_l, defined as

$$R_l = \frac{\Gamma_{had}}{\Gamma_{ll}}, \tag{5.24}$$

where $\Gamma_{had} = \sum_{q\neq t}\Gamma_{\bar{q}q}$ while Γ_{ee}, Γ_{ll} are the partial width of the Z into electrons and charged lepton respectively.
The observables Γ_{tot}, σ_{had} and R_l depend on the SMEFT Wilson coefficients only through the following linear combination:

$$\begin{aligned}\frac{l}{v^2} =&\left(-\frac{1}{4}+\frac{1}{3}\sin^2\theta_W\right)\cdot\left[(C_{\phi q}^{(1)})_{11}-(C_{\phi q}^{(3)})_{11}\right]+\left(-\frac{1}{3}-\frac{1}{6}\sin^2\theta_W\right)\cdot\left[(C_{\phi q}^{(1)})_{11}+(C_{\phi q}^{(3)})_{11}+\right.\\ &\left.+(C_{\phi q}^{(1)})_{22}+(C_{\phi q}^{(3)})_{22}\right]+\frac{1}{3}\sin^2\theta_W\cdot(C_{\phi u})_{11}-\frac{1}{6}\sin^2\theta_W\cdot\left[(C_{\phi d})_{11}+(C_{\phi d})_{22}\right].\end{aligned} \tag{5.25}$$

The value of l is constrained to lie with 95% probability in the interval [1]

$$-0.63\times10^{-3} < l < 1.2\times10^{-3}. \tag{5.26}$$

The second fit, performed on the coefficients of the operators with leptons and heavy quarks, involve all the observables at the Z pole and produces the following results:

$$-0.003 < v^2\left[(C_{\phi q}^{(1)})_{22}-(C_{\phi q}^{(3)})_{22}\right] < 0.01, \tag{5.27}$$

$$-0.01 < v^2(C_{\phi u})_{22} < 0.02, \tag{5.28}$$

$$-0.008 < v^2\left[(C_{\phi q}^{(1)})_{33}+(C_{\phi q}^{(3)})_{33}\right] < 0.002, \tag{5.29}$$

The study of the implications of bounds (5.26)–(5.29) on our model has been performed as follows:

1. The Wilson coefficients of the operators of interest, namely $C_{\phi q}^{(1)}$, $C_{\phi q}^{(3)}$, $C_{\phi u}$, $C_{\phi d}$ have been considered. They are generated at tree level by our VLQs, thus a tree-level matching on the NP scale Λ has been performed as explained in section 4.1.
2. These Wilson coefficients were run from the scale Λ down to the scale at which the bounds (5.26)–(5.29) are given, namely $\mu = M_Z$. Since these operators are generated at tree level at the scale Λ, we expect negligible effects due to the running.
   As for FCNC, we considered here the RG running contribution of Yukawa matrices, given in [64], in the LL approximation:

$$\begin{aligned}(C_{\phi q}^{(1)})_{pr}(\mu) =&(C_{\phi q}^{(1)})_{pr}(\Lambda)+\frac{1}{16\pi^2}\log\left(\frac{\mu}{\Lambda}\right)\cdot\left(-[Y_u^\dagger]_{ps}(C_{\phi u})_{st}[Y_u]_{tr}-[Y_d^\dagger]_{ps}(C_{\phi d})_{st}[Y_d]_{tr}\right.\\ &+\frac{3}{2}[Y_d^\dagger Y_d+Y_u^\dagger Y_u]_{pt}(C_{\phi q}^{(1)})_{tr}+\frac{3}{2}(C_{\phi q}^{(1)})_{pt}[Y_d^\dagger Y_d+Y_u^\dagger Y_u]_{tr}\\ &\left.+\frac{9}{2}[Y_d^\dagger Y_d-Y_u^\dagger Y_u]_{pt}(C_{\phi q}^{(3)})_{tr}+\frac{9}{2}(C_{\phi q}^{(3)})_{pt}[Y_d^\dagger Y_d-Y_u^\dagger Y_u]_{tr}\right)\end{aligned} \tag{5.30}$$

$$(C^{(3)}_{\phi q})_{pr}(\mu) = (C^{(3)}_{\phi q})_{pr}(\Lambda) + \frac{1}{16\pi^2}\log\left(\frac{\mu}{\Lambda}\right)\cdot\left(\frac{3}{2}[Y_d^\dagger Y_d - Y_u^\dagger Y_u]_{pt}(C^{(1)}_{\phi q})_{tr} + \frac{3}{2}(C^{(1)}_{\phi q})_{pt}[Y_d^\dagger Y_d - Y_u^\dagger Y_u]_{tr} + \frac{1}{2}[Y_d^\dagger Y_d + Y_u^\dagger Y_u]_{pt}(C^{(3)}_{\phi q})_{tr} + \frac{1}{2}(C^{(3)}_{\phi q})_{pt}[Y_d^\dagger Y_d + Y_u^\dagger Y_u]_{tr}\right) \tag{5.31}$$

$$(C_{\phi d})_{pr}(\mu) = (C_{\phi d})_{pr}(\Lambda) + \frac{1}{16\pi^2}\log\left(\frac{\mu}{\Lambda}\right)\cdot\left(-2[Y_d]_{ps}(C^{(1)}_{\phi q})_{st}[Y_d^\dagger]_{tr} + 3[Y_d Y_d^\dagger]_{pt}(C_{\phi d})_{tr} + 3(C_{\phi d})_{pt}[Y_d Y_d^\dagger]_{tr} - [Y_d Y_u^\dagger]_{pt}(C_{\phi ud})_{tr} - (C^*_{\phi ud})_{tp}[Y_u Y_d^\dagger]_{tr}\right) \tag{5.32}$$

$$(C_{\phi u})_{pr}(\mu) = (C_{\phi u})_{pr}(\Lambda) + \frac{1}{16\pi^2}\log\left(\frac{\mu}{\Lambda}\right)\cdot\left(-2[Y_u]_{ps}(C^{(1)}_{\phi q})_{st}[Y_u^\dagger]_{tr} + 3[Y_u Y_u^\dagger]_{pt}(C_{\phi u})_{tr} + 3(C_{\phi u})_{pt}[Y_u Y_u^\dagger]_{tr} - [Y_u Y_d^\dagger]_{pt}(C^*_{\phi ud})_{rt} - (C_{\phi ud})_{pt}[Y_d Y_u^\dagger]_{tr}.\right) \tag{5.33}$$

3. The elements $(C^{(1)}_{\phi q})_{11}$, $(C^{(1)}_{\phi q})_{22}$, $(C^{(1)}_{\phi q})_{33}$ $(C^{(3)}_{\phi q})_{11}$, $(C^{(3)}_{\phi q})_{22}$, $(C^{(3)}_{\phi q})_{33}$, $(C_{\phi u})_{11}$, $(C_{\phi u})_{22}$, $(C_{\phi d})_{11}$ and $(C_{\phi d})_{22}$ were computed with `Mathematica` within the same assumptions of the previous section, i.e. flavor diagonal and universal couplings $\lambda = 1$ and $M_a = \Lambda$ (with $a = U, D, Q_1$) while Λ was kept as parameter.
4. The linear combination l and the coefficients appearing in (5.27)–(5.29) were thus computed as a function of the NP scale Λ. The bounds (5.26)–(5.29) translate into bounds on Λ. In particular, for l three cases were considered:
   - Case a: with $\lambda_D, \lambda^d_Q = 0$ and $\lambda_U, \lambda^u_Q = 1$;
   - Case b: with $\lambda_D, \lambda^d_Q = 1$ and $\lambda_U, \lambda^u_Q = 0$;
   - Case c: with $\lambda_D, \lambda^d_Q = 1$ and $\lambda_U, \lambda^u_Q = 1$.

The results are shown in Table 5.2.

5.2.2 Bounds from the Peskin-Takeuchi parameters

Another way EWPT can test extensions of SM is through the Peskin-Takeuchi parameters S, T and U [78, 79], which parameterize potential new physics contributions to electroweak radiative corrections. The point $S = T = U = 0$ is defined with the top mass $m_t = 173$ GeV and the Higgs boson mass $m_h = 126$ GeV. Current experimental measurements [80] give

$$S = 0.02 \pm 0.07, \qquad T = 0.06 \pm 0.06, \tag{5.34}$$

with a correlation of 81%. This fit is illustrated in figure 5.5 and fixes $U = 0$. The S parameter is considered to be sensitive to the difference between the number of left-handed and right-handed fermions, whereas the T parameter is usually interpreted as a measure of custodial symmetry violation. In practice, S and T tend to give stronger constraints on BSM physics than U.
The standard operator based approach identifies the S parameter with the operator $Q_{\phi WB}$ and the T parameter with the operator $Q_{\phi D}$,

$$S = \frac{4scv^2}{\alpha}C_{\phi WB}, \qquad T = -v^2\frac{1}{2\alpha}C_{\phi D}, \tag{5.35}$$

where $\alpha = e^2/(4\pi)$ is evaluated at the energy scale of the Z-boson, namely $\alpha(M_Z) \approx (127.5)^{-1}$ [81], whereas $s = \sin\theta_W$ and $c = \cos\theta_W$.
We remind that neither of them are generated at tree level by our VLQs. To calculate the contribution of $C_{\phi WB}$ and $C_{\phi D}$ to S and T at the weak scale, we have to consider their RG evolutions [65]. The former does not contain contributions from our tree-level-generated operators, while the latter gets

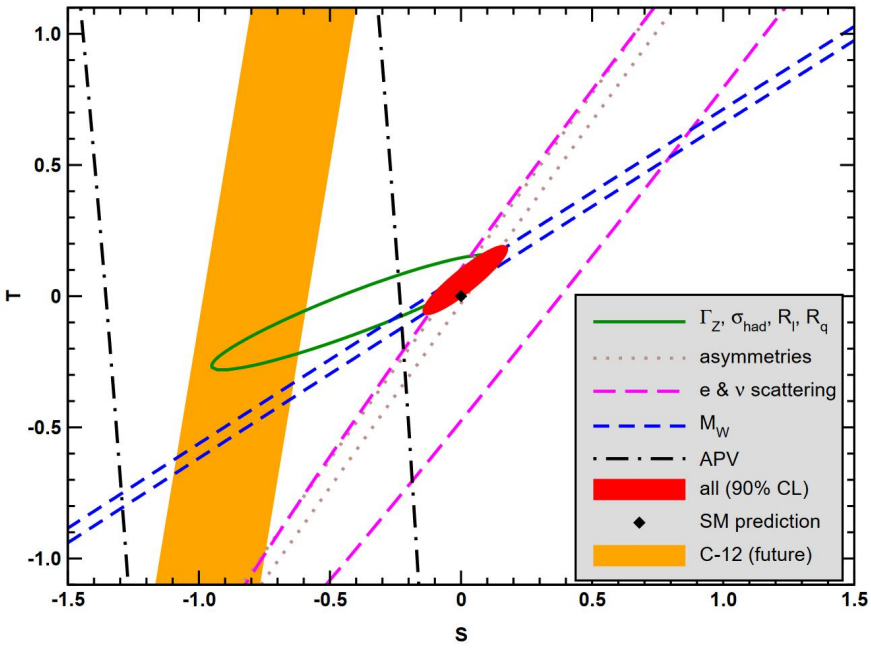

Figure 5.5: T versus S for various data set [80].

contributions from the mixing with $C_{\phi q}^{(1)}$, $C_{\phi u}$, $C_{\phi d}$ and $C_{\phi ud}$. Its RG equation [65] within the LL approximation reads

$$C_{\phi D} = \frac{g_1^2}{2\pi^2}\log\left(\frac{\mu}{\Lambda}\right)\cdot\left[-\frac{1}{3}(C_{\phi d})_{tt} + \frac{2}{3}(C_{\phi u})_{tt} + \frac{1}{3}(C_{\phi q}^{(1)})_{tt}\right] - 2\eta, \tag{5.36}$$

with t an index in the sum and

$$\begin{aligned}\eta =& \frac{1}{16\pi^2}\log\left(\frac{\mu}{\Lambda}\right)\Big(12(C_{\phi q}^{(1)})_{rs}[Y_d^\dagger Y_d - Y_u^\dagger Y_u]_{sr} + 12(C_{\phi u})_{rs}[Y_u Y_u^\dagger]_{sr} - 12(C_{\phi d})_{rs}[Y_d Y_d^\dagger]_{sr} \\ &+ 6(C_{\phi ud})_{rs}[Y_d Y_u^\dagger]_{sr} + 6(C_{\phi ud}^*)_{sr}[Y_u Y_d^\dagger]_{sr}\Big).\end{aligned} \tag{5.37}$$

As before, the value of T was computed with `Mathematica` assuming flavor diagonal and universal couplings $\lambda = 1$ and setting the masses of the VLQs equal to Λ. The consequent bound on the NP scale is reported in 5.2.

Constrained quantity	Bound on Λ
l (case a)	$\Lambda \gtrsim 3.47$ TeV
l (case b)	$\Lambda \gtrsim 4.9$ TeV
l (case c)	$\Lambda \gtrsim 6$ TeV
$(C_{\phi q}^{(1)})_{22} - (C_{\phi q}^{(3)})_{22}$	$\Lambda \gtrsim 1.74$ TeV
$(C_{\phi u})_{22}$	$\Lambda \gtrsim 1.74$ TeV
$(C_{\phi q}^{(1)})_{33} + (C_{\phi q}^{(3)})_{33}$	$\Lambda \gtrsim 2.39$ TeV
T	$\Lambda \gtrsim 0.09$ TeV

Table 5.2: Bounds on Λ from EWPT constraints, up basis.

Remarkably, the strongest bound is provided by the limit on l, particularly by the case with both the up-type and the down-type VLQs interactions are turned on, which is is clearly understood when looking at its expression.

5.3 Higgs Physics

The production mechanisms at the Tevatron collider and the LHC, as portrayed in the left side of figure 5.6, are gluon fusion (ggF), weak-boson fusion (VBF), associated production with a gauge boson (Vh), associated production with a top or bottom quark pair ($t\bar{t}h$ and $b\bar{b}h$ respectively) and associated production with a single top quark (th).
The Higgs boson decays into heavy vector boson pairs, fermion-antifermion pairs, and photon/Z-boson pairs (see figure 5.6, right). The discovery of the Higgs boson was made essentially through bosonic final states. These decays probed mostly the couplings of the Higgs boson to vector bosons.
However, the predominant Higgs boson production mode is the gluon fusion, occurring only through loops dominated by the coupling of the Higgs boson to fermions. The observation of the Higgs boson in the two photons or two gluons decay modes is also an indirect evidence for the coupling of the Higgs boson to fermions (and in particular to the top quark). Nevertheless, the observation of either decays to fermions or production modes which unambiguously proceed through fermion couplings provide direct probes of the coupling of the Higgs boson to fermions.
In the next sections we consider the existing experimental bounds on the Higgs couplings to the top quark and the bottom quark, and to gluons/photons. We do not consider the couplings to the vector bosons or leptons since our NP does not modify them.

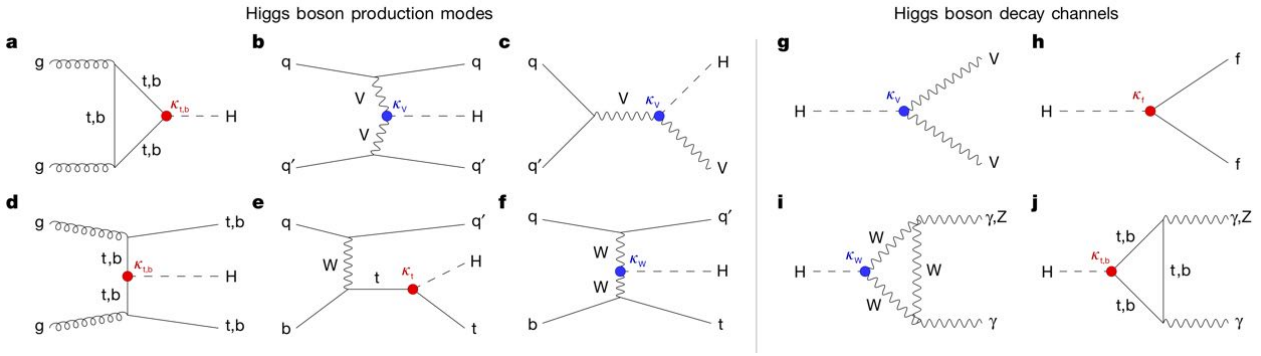

Figure 5.6: Production mechanisms (left): a) ggF, b) VBF, c) Vh, d) $t\bar{t}h$, $b\bar{b}h$ e,f) th.
Decay mechanisms (right): g) Higgs to vector bosons, h) Higgs to fermion pair, i,j) Higgs to γ, Z. Figure from [4].

5.3.1 Higgs to top and bottom

The coupling of the Higgs boson to the bottom quark is directly provided by the measurements of the $h \to b\bar{b}$, which occurs at tree level (see figure 5.6, diagram h). For a Higgs boson with $m_h \sim 125$ GeV, the branching fraction to $b\bar{b}$ is about 58% [82], but the presence of very large backgrounds makes the isolation of a Higgs boson signal in these channels quite challenging. In the search for the decay of the Higgs boson to a pair of b-quarks, the most sensitive production modes are the associated WH and ZH processes which can be triggered by the leptonic decays of W and Z, but ATLAS and CMS have also searched for $h \to b\bar{b}$ in the VBF production mode.
The direct observation of the Higgs boson decaying to a pair of b-quarks was obtained by both ATLAS and CMS independently via the analysis of a impressive dataset collected in 2015, 2016 and 2017. These results provided direct evidence for the $h \to b\bar{b}$ decay through the VH production mode.

In the case of the top quark, the direct decay $h \to t\bar{t}$ cannot occur due to kinematical reasons. However, indirect evidence of this coupling is provided by the compatibility of observed rates of the Higgs boson in the principal discovery channels, given that the main production process – the gluon fusion – is dominated by a top quark loop (figure 5.6, diagram a).
Direct evidence of this coupling at the LHC and the future e^+e^- colliders will be mainly available through the ttH final state and will permit a clean measurement of the top quark-Higgs boson Yukawa coupling.

Currently, the existing bounds on the coupling strenght modifiers κ_b and κ_t, defined in (5.41), are [4]:

$$0.83 < \kappa_b < 1.16, \qquad 0.91 < \kappa_t < 1.12. \tag{5.38}$$

In terms of the effective operators $C_{u\phi}, C_{d\phi}$, which modify the Yukawa couplings, we have

$$\kappa_\star = \frac{g_{h\star}}{g_{h\star}^{SM}} = \frac{\frac{m_\star}{v} - \frac{1}{\sqrt{2}} v^2 C_{\star\phi}}{\frac{m_\star}{v}} \qquad \text{with } \star = b, t. \tag{5.39}$$

where with $C_{b\phi}$ and $C_{t\phi}$ we mean $(C_{d\phi})_{33}$ and $(C_{u\phi})_{33}$, respectively. By exploiting the matching conditions in 4.5, we can constrain our NP model via the Wilson coefficients. As previously done, we set the couplings λ_i to 1 and the masses of the VLQs to Λ.
Thus, the limits (5.38) translate into bounds on Λ with 95% probability:

$$\text{for } \kappa_b \to \Lambda \gtrsim 2.73 \text{ TeV}, \qquad \text{for } \kappa_t \to \Lambda \gtrsim 0.033 \text{ TeV}. \tag{5.40}$$

We can observe that, despite having similar uncertainties, the coupling strength modifier related to the bottom quark is much more constraining than the one of the top quark. This is due to the fact that, in a universally enhanced Yukawa paradigm, the bottom quark coupling is much more modified than the top quark one, due to their difference of masses [8].

5.3.2 Higgs to gluons and photons

The effective coupling of the Higgs to gluons has been constrained by the measurements carried out at LHC by the CMS and ATLAS collaborations. The constraint is given in terms of the modifier κ_g, defined as

$$\kappa_g = \frac{|\mathcal{M}_{SM} + \mathcal{M}_{NP}|^2}{|\mathcal{M}_{SM}|^2}. \tag{5.41}$$

The experimental constraint on κ_g is obtained from single Higgs production processes and reads [4]

$$\kappa_g = 0.92 \pm 0.08. \tag{5.42}$$

These constraints come from the analysis of processes involving a gluon-gluon single-Higgs production. From the theoretical point of view, this process can occur via the following diagrams:

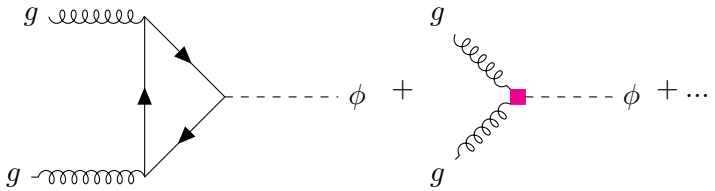

The SM production occurs via the triangle loop in which mainly a virtual top circulates, while the contributions from NP can be relevant for the single Higgs production in two ways:

- via the modification of the top Yukawa coupling;
- with the effective interaction hgg, which in our case can be generated at high energy by the circulation of the VLQs in the triangle loop.

To put a constraint on our model, let us translate the bounds on κ_g into bounds on the effective operators, in a model-independent approach. On this purpose, we consider the operators

$$Q_{t\phi} = (Q_{u\phi})_{33} = (\phi^\dagger \phi)(\bar{Q}_L \tilde{\phi} t_R), \tag{5.43}$$

$$Q_{\phi G} = G^a_{\mu\nu} G^{a\mu\nu} \phi^\dagger \phi. \tag{5.44}$$

As seen in the previous section, the first operator modifies the top Yukawa coupling, while the second operator describes the effective interaction between two gluons and two Higgs doublets (see the right-hand side of 5.7).
As it becomes clear once we move to the broken phase, the $Q_{\phi G}$ operator includes the effective interaction between two gluons and one Higgs boson. Indeed:

$$\frac{C_{\phi G}}{\Lambda^2} G^a_{\mu\nu} G^{a\mu\nu} \phi^\dagger \phi \to \frac{C_{\phi G}}{\Lambda^2} G^a_{\mu\nu} G^{a\mu\nu} v^2 \left(\frac{1}{2} + \frac{h}{v} + \frac{h^2}{2v^2} \right). \tag{5.45}$$

In the case of single Higgs production, the relevant effective operators can be rewritten as:

$$\frac{C_{u\phi}}{\Lambda^2} Q_{u\phi} \to c_1 \frac{m_t}{v} h \bar{t} t \qquad \text{with } c_1 = 1 - \frac{v}{m_t} \cdot \frac{1}{\sqrt{2}} \frac{v^2}{\Lambda^2} C_{t\phi}, \tag{5.46}$$

$$\frac{C_{\phi G}}{\Lambda^2} Q_{\phi G} \to c_2 \frac{\alpha_s}{\pi v} h G^a_{\mu\nu} G^{a\mu\nu} \qquad \text{with } c_2 = \frac{C_{\phi G}}{\Lambda^2} \cdot \frac{v^2 \pi}{\alpha_s}. \tag{5.47}$$

The LO matrix element for the process $gg \to h$ can be decomposed in [83]

$$\mathcal{M}_{gg\to h}(p_1, p_2) = i \frac{\alpha_s}{3\pi v} \epsilon_\mu(p_1) \epsilon_\nu(p_2) [p_1^\nu p_2^\mu - (p_1 \cdot p_2) g^{\mu\nu}] F(x_H), \tag{5.48}$$

where p_1, p_2 are the gluon momenta, $\epsilon(p_1), \epsilon(p_2)$ are their polarizations and $x_H = 4m_t^2/m_h^2$. The form factor $F(x)$ is defined as

$$F(x) = c_1 \cdot F_1(x) + c_2 \cdot F_2(x), \tag{5.49}$$

with

$$F_1(x) = \frac{3}{2} x [1 + (1 - x) f(x)], \tag{5.50}$$

$$F_2(x) = 12. \tag{5.51}$$

The function f is defined as

$$f(x) = \begin{cases} \arcsin^2 \dfrac{1}{\sqrt{x}}, & \text{for } x \geq 1 \\ -\dfrac{1}{4} \left[\log \dfrac{1 + \sqrt{1 - x}}{1 - \sqrt{1 - x}} - i\pi \right]^2, & \text{for } x < 1 \end{cases} \tag{5.52}$$

The coefficient c_1 describes modifications of the $t\bar{t}h$ coupling, so the pure SM contribution is obtained by setting $c_1 = 1$ and $c_2 = 0$. Thus, we can translate the bound on κ_g to a bound on c_1, c_2 via the following relation obtained from (5.41)

$$\kappa_g = \frac{|c_1 \cdot F_1 + c_2 \cdot F_2|^2}{|F_1|^2} = c_1^2 + 2 \frac{F_2}{F_1} \cdot c_1 \cdot c_2 + \frac{F_2^2}{F_1^2} \cdot c_2^2, \tag{5.53}$$

where the second equality holds since we are dealing with real quantities.
In turn, a bound on c_1, c_2 means a bound on $C_{\phi G}$, $C_{t\phi}$, which allows to constrain our specific model. On this purpose, a matching of $C_{\phi G}$ coefficient is needed. To perfom this matching, which is represented by diagrams in figure 5.7, a previous calculation was used [84]. In this work, the effective interaction between two gluons and two Higgs boson is described by the Lagrangian term

$$\mathcal{L}_{hhgg} = \frac{g_s^2}{96\pi^2 v^2} K_{2g} G^a_{\mu\nu} G^{a\mu\nu} h^2. \tag{5.54}$$

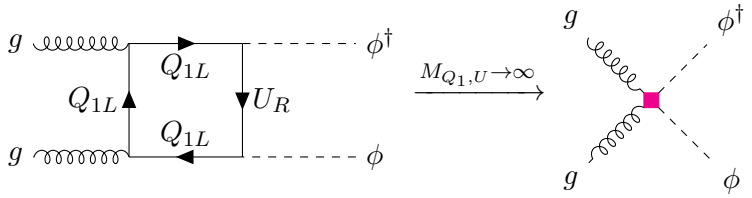

Figure 5.7: The effective operator $Q_{\phi G}$ can be generated at loop-level in the underlying heavy theory involving exchange of heavy VLQs as depicted in the diagram on the left.

The Feynman amplitudes are calculated in the broken phase:

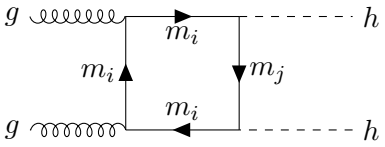

$$\mathcal{A} = \frac{\alpha_s}{4\pi}\delta^{ab}\epsilon^a_\mu\epsilon^b_\nu(-s)A_1^{\mu\nu}\cdot\sum_{i,j=1}^{4} g^2_{h\bar{q}_i q_j}F_\square(m_i,m_j), \tag{5.55}$$

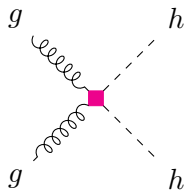

$$\mathcal{A} = \frac{\alpha_s}{3\pi v^2}\delta^{ab}\epsilon^a_\mu\epsilon^b_\nu A_1^{\mu\nu}\cdot K_{2g}. \tag{5.56}$$

where

- $A_1^{\mu\nu} = p_1^\nu p_2^\mu - p_1\cdot p_2 g^{\mu\nu}$ with p_1, p_2 the gluon momenta;
- $g_{h\bar{q}_i q_j} = \frac{1}{2}(\lambda_{hff,ij} + \lambda_{hff,ji})$ with $\lambda_{hff,ij}$ the (ith,jth) matrix element of the coupling matrix in the mass eigenstate basis.

In the large quark mass limit for $m_i = m_j$ the form factor reduces to $F_\square = -2s/(3m_i^2)$.
Then, by comparing equations (5.55) and (5.56) we obtain the matching condition on K_{2g}:

$$K_{2g} = \frac{v^2}{2}\sum_{i,j=1}^{4}\frac{g^2_{h\bar{q}_i q_j}}{m_i^2}. \tag{5.57}$$

The last step is to relate the K_{2g} coupling, which is specific for the $hhgg$ interaction, to the $C_{\phi G}$ operator. This is quickly done by comparing the terms of interest in equations (5.45) and (5.54). This implies

$$\frac{C_{\phi G}}{\Lambda^2} = \frac{g_s^2}{48\pi^2 v^2}\cdot K_{2g} = \frac{g_s^2}{96\pi^2}\sum_{A=U,D}\frac{(\lambda_{AQ_1})^2}{M^2_{VLQ}}. \tag{5.58}$$

In the last equality we assumed for simplicity real and flavor diagonal $\lambda_{DQ_1}, \lambda_{UQ_1}$ and $M_{Q_1} = M_U = M_D = M_{VLQ}$, thus the terms in the sum are all equal. The possible combinations are depicted in figure 5.8, for a total of 8 possibilities. At this point, by exploiting the matching relations for the Wilson coefficients $C_{t\phi}, C_{\phi G}$, we can express κ_g in terms of our UV parameters, namely the couplings λ_i and the masses of the VLQs. As before, we choose to set all the new couplings to 1 and $M_{VLQ} = \Lambda$. Thus a bound on the NP energy scale is obtained with 95% probability:

$$\Lambda \gtrsim 2.74 \text{ TeV}. \tag{5.59}$$

Notice that with the assumption of having only the top quark circulating in the triangle among the SM quarks, we are neglecting the contributions from the bottom quark. However, by neglecting this contribution both on the numerator and the denominator of 5.41, the committed error is minimal.
For what concerns the coupling of the Higgs to photons, the effect of the VLQs again is minimal since the Higgs boson to photons is dominated by W bosons loop (see figure 5.6, diagram i). Since our

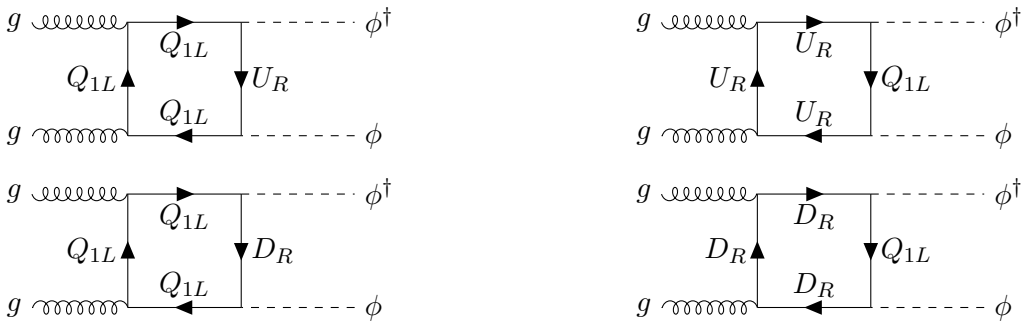

+ diagrams with opposite fermion flow.

Figure 5.8: Possible combinations of VLQs running in the box loop for the $gg \to \phi\phi$ process.

NP model does not influence this loop, the effect on κ_γ is smaller than the experimental error on κ_γ. For this reason, we can safely assume the experimental constraint on $h\gamma\gamma$ is not providing a bound stronger than the one from hgg.

Chapter 6

Results and conclusions

The aim of this work was to build a model in which large enhancements of the light quark Yukawa couplings are concretely realized. In particular we tried to answer the question *"how large can the light quark Yukawa couplings be?"*

In order to answer the question a concrete model of NP was considered. The model was identified to be among the class of models that generate tree-level contributions to the dimension-six operators $Q_{u\phi}$ and $Q_{d\phi}$ when matched to the SMEFT. Those operators are the equivalent to the SM Yukawa couplings but containing an additional $\phi^\dagger\phi$. While there exists a huge plethora of models that get contributions to this operators by tree-level matching, we identify the ones with vector-like quarks as being the most promising ones as they do not suffer from Yukawa suppression. Given this, we studied an example case in which the VLQs are heavier copies of the right-handed up-type or respectively down-type quarks as well as the left-handed SU(2) doublet quark fields. The NP contributions were parameterized within the SMEFT, which was then exploited to connect the UV theory to the experimental bounds. In this way, it was possible to constrain our NP model from lower energy probes such as the ones stemming from flavour physics, electroweak precision tests and Higgs physics making use of the RGE running and operator mixing within the SMEFT. In particular we could constrain the NP energy scale Λ identified as the mass of the VLQ. Here we present our results in light of these bounds, which are summarized in fig. 6.1. The plots show the coupling strength modifiers κ_i with $i = u, d$ as function of the mass of the VLQs. The vertical lines represent the constraints on $M_{VLQ} = \Lambda$ obtained from the considered experimental bounds, namely FCNC (pink dashed line), EWPT (red dashed line) and Higgs physics (green dashed line), by setting the couplings λ to 1, while the horizontal line represents the projected sensitivity on κ_i from off-shell Higgs production from ref. [37]. The plots present a scenario in which both right-handed up-and down-type VLQs are present. The strongest limit is imposed by EWPT ($\Lambda \gtrsim 6$ TeV). For this value of Λ the coupling strength modifiers are $\kappa_u \sim 128$ and $\kappa_d \sim 62$, so the enhancement can be moderately realized. We note though, that in particular the bounds from EWPTs become weaker in scenarios were only either down- or up-type singlet VLQs are present. In this case one can though obtain large modifications only either for the light down-type or up-type quarks.

Keeping in mind that the purpose of the thesis was to answer the question on how large the enhancements of the light quark Yukawa couplings get, we did not attempt to solve any of the open puzzles of the SM by means of adding the VLQs. In general, VLQs are the ingredient of various BSM theories, which try to address one or more of these open puzzles. In such a framework, the simplified model solution proposed in this thesis might be realised and lead to strongly enhanced light quark Yukawa couplings, requiring to test such scenarios in experiments. We note also that the proposed NP theory may not be the most attractive due to the non-negligible amount of tuning which is required to fix the mass value of the light quark while having an increased coupling to the Higgs boson. Nevertheless, the obtained result gives an indication of the range of coupling values that experimental probes of the light quark Yukawa couplings should aim for. Indeed, we demonstrate that it is possible to realise by 2–3 orders of magnitude enhanced light quark Yukawa. While current proposals to probe this couplings

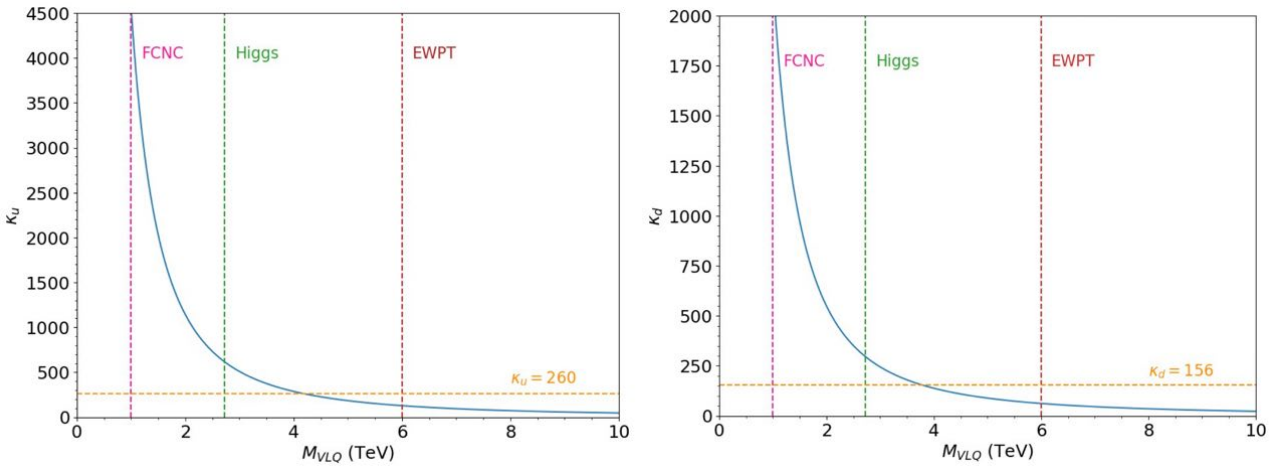

Figure 6.1: On the vertical axis, the coupling strength modifier κ for the up quark (left) and the down quark (right) are shown, while the horizontal axis shows the masses of the VLQs. In these plots the couplings λ were set to 1. The experimental constraints on Λ are shown, in particular from EWPT (red line), from Higgs physics (green line) and from FCNC (pink line). The horizontal lines describe the HL-LHC projected sensitivity on κ_i, taken from [37].

at the HL-LHC seem not to be reaching this interesting parameter space just yet, this work indicates that at least we might be probing an interesting order of magnitude that can be explicitly realised in concrete models. The provided range might also provide a physics case for future collider facilities.

For future work, it might be interesting to explore alternative flavour structures, motivated by the fact that so far the FCNC constrains seem to be much weaker as the ones from EWPTs. In addition, it might be interesting to study $\Delta F = 1$ processes to which also non-logarithmic contributions might be relevant. Furthermore, it might be useful to systematically study other combinations of VLQs appearing in table 3.2 to get a more systematic answer of our initial question.
While the analysis has been performed within a SMEFT framework, which seems justified in retroperspective given the rather large NP scale Λ, it might anyways be interesting to confront concrete model predictions with their SMEFT counterparts. In the former case, further experimental constrains might be relevant such as for instance the unitarity of the CKM matrix V_{CKM}.

Bibliography

[1] R. Contino, M. Ghezzi, C. Grojean, M. Muhlleitner, and M. Spira, "Effective Lagrangian for a light Higgs-like scalar," *JHEP* **07** (2013) 035, arXiv:1303.3876 [hep-ph].

[2] L. Silvestrini and M. Valli, "Model-independent Bounds on the Standard Model Effective Theory from Flavour Physics," *Phys. Lett. B* **799** (2019) 135062, arXiv:1812.10913 [hep-ph].

[3] **ATLAS** Collaboration, "A detailed map of Higgs boson interactions by the ATLAS experiment ten years after the discovery," *Nature* **607** no. 7917, (2022) 52–59, arXiv:2207.00092 [hep-ex]. [Erratum: Nature 612, E24 (2022)].

[4] **CMS** Collaboration, A. Tumasyan *et al.*, "A portrait of the Higgs boson by the CMS experiment ten years after the discovery," *Nature* **607** no. 7917, (2022) 60–68, arXiv:2207.00043 [hep-ex].

[5] S. Weinberg, "A model of leptons," *Phys. Rev. Lett.* **19** (Nov, 1967) 1264–1266. https://link.aps.org/doi/10.1103/PhysRevLett.19.1264.

[6] A. Salam, "Proceedings of the 8th nobel symposium," *Almquist & Wiskell, Stockholm* (1968) .

[7] S. L. Glashow, "Partial-symmetries of weak interactions," *Nuclear Physics* **22** no. 4, (1961) 579–588. https://www.sciencedirect.com/science/article/pii/0029558261904692.

[8] **Particle Data Group** Collaboration, R. L. Workman and Others, "Review of Particle Physics," *PTEP* **2022** (2022) 083C01.

[9] P. W. Higgs, "Broken symmetries and the masses of gauge bosons," *Phys. Rev. Lett.* **13** (Oct, 1964) 508–509. https://link.aps.org/doi/10.1103/PhysRevLett.13.508.

[10] P. Higgs, "Broken symmetries, massless particles and gauge fields," *Physics Letters* **12** no. 2, (1964) 132–133. https://www.sciencedirect.com/science/article/pii/0031916364911369.

[11] F. Englert and R. Brout, "Broken symmetry and the mass of gauge vector mesons," *Phys. Rev. Lett.* **13** (Aug, 1964) 321–323. https://link.aps.org/doi/10.1103/PhysRevLett.13.321.

[12] A. Djouadi, "The Anatomy of electro-weak symmetry breaking. I: The Higgs boson in the standard model," *Phys. Rept.* **457** (2008) 1–216, arXiv:hep-ph/0503172.

[13] M. Kobayashi and T. Maskawa, "CP-Violation in the Renormalizable Theory of Weak Interaction," *Progress of Theoretical Physics* **49** no. 2, (02, 1973) 652–657, https://academic.oup.com/ptp/article-pdf/49/2/652/5257692/49-2-652.pdf. https://doi.org/10.1143/PTP.49.652.

[14] Z. Maki, M. Nakagawa, and S. Sakata, "Remarks on the Unified Model of Elementary Particles," *Progress of Theoretical Physics* **28** no. 5, (11, 1962) 870–880, https://academic.oup.com/ptp/article-pdf/28/5/870/5258750/28-5-870.pdf. https://doi.org/10.1143/PTP.28.870.

[15] G. Aad, T. Abajyan, B. Abbott, J. Abdallah, S. A. Khalek, A. A. Abdelalim, R. Aben, B. Abi, M. Abolins, O. AbouZeid, *et al.*, "Observation of a new particle in the search for the standard model higgs boson with the atlas detector at the lhc," *Physics Letters B* **716** no. 1, (2012) 1–29.

[16] **CMS** Collaboration, S. Chatrchyan *et al.*, "Observation of a New Boson at a Mass of 125 GeV with the CMS Experiment at the LHC," *Phys. Lett. B* **716** (2012) 30–61, arXiv:1207.7235 [hep-ex].

[17] **LHC Higgs Cross Section Working Group** Collaboration, J. R. Andersen *et al.*, "Handbook of LHC Higgs Cross Sections: 3. Higgs Properties," arXiv:1307.1347 [hep-ph].

[18] T. Barklow, K. Fujii, S. Jung, R. Karl, J. List, T. Ogawa, M. E. Peskin, and J. Tian, "Improved Formalism for Precision Higgs Coupling Fits," *Phys. Rev. D* **97** no. 5, (2018) 053003, arXiv:1708.08912 [hep-ph].

[19] **ATLAS** Collaboration, G. Aad *et al.*, "Direct constraint on the Higgs-charm coupling from a search for Higgs boson decays into charm quarks with the ATLAS detector," *Eur. Phys. J. C* **82** (2022) 717, arXiv:2201.11428 [hep-ex].

[20] **CMS** Collaboration, A. M. Sirunyan *et al.*, "A search for the standard model Higgs boson decaying to charm quarks," *JHEP* **03** (2020) 131, arXiv:1912.01662 [hep-ex].

[21] G. Perez, Y. Soreq, E. Stamou, and K. Tobioka, "Prospects for measuring the higgs boson coupling to light quarks," *Phys. Rev. D* **93** (Jan, 2016) 013001. https://link.aps.org/doi/10.1103/PhysRevD.93.013001.

[22] G. T. Bodwin, F. Petriello, S. Stoynev, and M. Velasco, "Higgs boson decays to quarkonia and the hcc coupling," *Phys. Rev. D* **88** no. 5, (2013) 053003, arXiv:1306.5770 [hep-ph].

[23] M. König and M. Neubert, "Exclusive radiative higgs decays as probes of light-quark yukawa couplings," *JHEP* **08** (2015) 012, arXiv:1505.03870 [hep-ph].

[24] S. Alte, M. König, and M. Neubert, "Exclusive weak radiative higgs decays in the standard model and beyond," *JHEP* **12** (2016) 037, arXiv:1609.06310 [hep-ph].

[25] A. L. Kagan, G. Perez, F. Petriello, Y. Soreq, S. Stoynev, and J. Zupan, "Exclusive window onto higgs yukawa couplings," *Phys. Rev. Lett.* **114** no. 10, (2015) 101802, arXiv:1406.1722 [hep-ph].

[26] J. Duarte-Campderros, G. Perez, M. Schlaffer, and A. Soffer, "Probing the higgs–strange-quark coupling at e^+e^- colliders using light-jet flavor tagging," *Phys. Rev. D* **101** (Jun, 2020) 115005. https://link.aps.org/doi/10.1103/PhysRevD.101.115005.

[27] J. A. Aguilar-Saavedra, J. M. Cano, and J. M. No, "More light on higgs flavor at the lhc: Higgs boson couplings to light quarks through $h + \gamma$ production," *Phys. Rev. D* **103** (May, 2021) 095023. https://link.aps.org/doi/10.1103/PhysRevD.103.095023.

[28] Y. Soreq, H. X. Zhu, and J. Zupan, "Light quark Yukawa couplings from Higgs kinematics," *JHEP* **12** (2016) 045, arXiv:1606.09621 [hep-ph].

[29] G. Bonner and H. E. Logan, "Constraining the Higgs couplings to up and down quarks using production kinematics at the CERN Large Hadron Collider," arXiv:1608.04376 [hep-ph].

[30] L. Alasfar, R. Corral Lopez, and R. Gröber, "Probing Higgs couplings to light quarks via Higgs pair production," *JHEP* **11** (2019) 088, arXiv:1909.05279 [hep-ph].

[31] L. Alasfar, R. Gröber, C. Grojean, A. Paul, and Z. Qian, "Machine learning the trilinear and light-quark Yukawa couplings from Higgs pair kinematic shapes," *JHEP* **11** (2022) 045, arXiv:2207.04157 [hep-ph].

[32] N. Vignaroli, "Off-Shell Probes of the Higgs Yukawa Couplings: Light Quarks and Charm," *Symmetry* **14** no. 6, (2022) 1183, arXiv:2205.09449 [hep-ph].

[33] A. Falkowski, S. Ganguly, P. Gras, J. M. No, K. Tobioka, N. Vignaroli, and T. You, "Light quark Yukawas in triboson final states," *JHEP* **04** (2021) 023, arXiv:2011.09551 [hep-ph].

[34] F. Yu, "Light quark yukawa couplings and the w±h charge asymmetry," *Nuclear and Particle Physics Proceedings* **285-286** (2017) 123–125. https://www.sciencedirect.com/science/article/pii/S2405601417300780. Sixth Workshop on Theory, Phenomenology and Experiments in Flavour Physics Interplay of Flavour Physics with Electroweak symmetry breaking.

[35] F. Yu, "Phenomenology of Enhanced Light Quark Yukawa Couplings and the $W^{\pm}h$ Charge Asymmetry," *JHEP* **02** (2017) 083, arXiv:1609.06592 [hep-ph].

[36] J. de Blas *et al.*, "Higgs Boson Studies at Future Particle Colliders," *JHEP* **01** (2020) 139, arXiv:1905.03764 [hep-ph].

[37] E. Balzani, R. Gröber, and M. Vitti, "Light-quark Yukawa couplings from off-shell Higgs production," arXiv:2304.09772 [hep-ph].

[38] E. Fermi, "Über die bildung von langsamen neutronen durch kernstöße," *Zeitschrift für Physik* **88** (1934) 161.

[39] E. E. Jenkins, A. V. Manohar, and P. Stoffer, "Low-energy effective field theory below the electroweak scale: Operators and matching," *Journal of High Energy Physics* **2018** no. 3, (2018) 016, arXiv:1709.04486 [hep-ph].

[40] E. E. Jenkins, A. V. Manohar, and P. Stoffer, "One-loop matching and running in the electroweak effective theory," *Journal of High Energy Physics* **2018** no. 1, (2018) 084, arXiv:1711.05270 [hep-ph].

[41] A. Pich, "Effective field theory: Course," *Reports on Progress in Physics* **58** (1995) 563, arXiv:hep-ph/9502366. https://iopscience.iop.org/article/10.1088/0034-4885/58/6/001.

[42] A. Pich, "Les houches summer school: Eft in particle physics and cosmology," *Les Houches Summer School Proceedings* (2018) , arXiv:1804.05664 [hep-ph]. Proceedings of the Les Houches Summer School on EFT in Particle Physics and Cosmology, Les Houches, Chamonix Valley, France, July 3-28, 2017.

[43] A. V. Manohar and M. B. Wise, *Cambridge Monographs on Particle Physics, Nuclear Physics and Cosmology*, vol. 10 of *Cambridge Monographs on Particle Physics, Nuclear Physics and Cosmology*. Cambridge University Press, 2000.

[44] I. Brivio and M. Trott, "The Standard Model as an Effective Field Theory," *Phys. Rept.* **793** (2019) 1–98, arXiv:1706.08945 [hep-ph].

[45] W. Buchmüller and D. Wyler, "Effective lagrangian analysis of new interactions and flavor conservation," *Nuclear Physics B* **268** (1986) 621.

[46] B. Grzadkowski, M. Iskrzynski, M. Misiak, and J. Rosiek, "Dimension-six terms in the standard model lagrangian," *Journal of High Energy Physics* **2010** no. 10, (2010) 085, arXiv:1008.4884 [hep-ph].

[47] A. Dedes, W. Materkowska, M. Paraskevas, J. Rosiek, and K. Suxho, "Feynman rules for the Standard Model Effective Field Theory in R_ξ -gauges," *JHEP* **06** (2017) 143, arXiv:1704.03888 [hep-ph].

[48] R. Rahman, "Higher Spin Theory - Part I," *PoS* **ModaveVIII** (2012) 004, arXiv:1307.3199 [hep-th].

[49] J. de Blas, J. C. Criado, M. Perez-Victoria, and J. Santiago, "Effective description of general extensions of the Standard Model: the complete tree-level dictionary," *JHEP* **03** (2018) 109, arXiv:1711.10391 [hep-ph].

[50] A. Djouadi and A. Lenz, "Sealing the fate of a fourth generation of fermions," *Phys. Lett. B* **715** (2012) 310–314, arXiv:1204.1252 [hep-ph].

[51] G. Aad *et al.*, "ATLAS-CONF-2013-034," tech. rep., ATLAS Collaboration, 2013.

[52] S. Chatrchyan *et al.*, "CMS-PAS-HIG-13-005," tech. rep., CMS Collaboration, 2013.

[53] **ATLAS** Collaboration, G. Aad *et al.*, "Search for pair production of heavy top-like quarks decaying to a high-pT W boson and a b quark in the lepton plus jets final state at $\sqrt{s}$=7 TeV with the ATLAS detector," *Phys. Lett. B* **718** (2013) 1284–1302, arXiv:1210.5468 [hep-ex].

[54] **CMS** Collaboration, S. Chatrchyan *et al.*, "Search for Pair Produced Fourth-Generation Up-Type Quarks in pp Collisions at $\sqrt{s} = 7$ TeV with a Lepton in the Final State," *Phys. Lett. B* **718** (2012) 307–328, arXiv:1209.0471 [hep-ex].

[55] F. del Aguila and M. J. Bowick, "Nucl. phys. b 224 (1983) 107," *Nuclear Physics B* **224** (1983) 107.

[56] G. C. Branco and L. Lavoura, "Nucl. phys. b 278 (1986) 738," *Nuclear Physics B* **278** (1986) 738.

[57] Y. Nir and D. J. Silverman, "Phys. rev. d 42 (1990) 1477," *Physical Review D* **42** (1990) 1477.

[58] G. Barenboim, F. J. Botella, G. C. Branco, and O. Vives, "Phys. lett. b 422 (1998) 277," *Physics Letters B* **422** (1998) 277, hep-ph/9709369.

[59] S. Bar-Shalom, A. Soni, and J. Wudka, "Effective field theory analysis of Higgs naturalness," *Phys. Rev. D* **92** no. 1, (2015) 015018, arXiv:1405.2924 [hep-ph].

[60] K. S. Babu, I. Gogoladze, M. U. Rehman, and Q. Shafi, "Higgs Boson Mass, Sparticle Spectrum and Little Hierarchy Problem in Extended MSSM," *Phys. Rev. D* **78** (2008) 055017, arXiv:0807.3055 [hep-ph].

[61] M. Schmaltz and D. Tucker-Smith, "Ann. rev. nucl. part. sci. 55 (2005) 229," *Annual Review of Nuclear and Particle Science* **55** (2005) 229, hep-ph/0502182. and references therein.

[62] C. Delaunay, C. Grojean, and G. Perez, "Modified Higgs Physics from Composite Light Flavors," *JHEP* **09** (2013) 090, arXiv:1303.5701 [hep-ph].

[63] E. E. Jenkins, A. V. Manohar, and M. Trott, "Renormalization Group Evolution of the Standard Model Dimension Six Operators I: Formalism and lambda Dependence," *JHEP* **10** (2013) 087, arXiv:1308.2627 [hep-ph].

[64] E. E. Jenkins, A. V. Manohar, and M. Trott, "Renormalization Group Evolution of the Standard Model Dimension Six Operators II: Yukawa Dependence," *JHEP* **01** (2014) 035, arXiv:1310.4838 [hep-ph].

[65] R. Alonso, E. E. Jenkins, A. V. Manohar, and M. Trott, "Renormalization Group Evolution of the Standard Model Dimension Six Operators III: Gauge Coupling Dependence and Phenomenology," *JHEP* **04** (2014) 159, arXiv:1312.2014 [hep-ph].

[66] R. Alonso, H.-M. Chang, E. E. Jenkins, A. V. Manohar, and B. Shotwell, "Renormalization group evolution of dimension-six baryon number violating operators," *Phys. Lett. B* **734** (2014) 302–307, arXiv:1405.0486 [hep-ph].

[67] K. G. Wilson, "Phys. rev. b4, 3174 (1971)," *Physical Review B* **4** (1971) 3174.

[68] K. G. Wilson, "Phys. rev. b4, 3184 (1971)," *Physical Review B* **4** (1971) 3184.

[69] S. Glashow, J. Iliopoulos, and L. Maiani, "Weak interactions with lepton–hadron symmetry," *Physical Review D* **2** no. 7, (1970) 1285.

[70] M. Ciuchini, E. Franco, V. Lubicz, G. Martinelli, I. Scimemi, and et al., "Next-to-leading order qcd corrections to $\delta f = 2$ effective hamiltonians," *Nuclear Physics B* **523** (1998) 501–525, hep-ph/9711402.

[71] J. Aebischer, C. Bobeth, A. J. Buras, and J. Kumar, "SMEFT ATLAS of ΔF = 2 transitions," *JHEP* **12** (2020) 187, arXiv:2009.07276 [hep-ph].

[72] A. J. Buras, M. Misiak, and J. Urban, "Two-loop qcd anomalous dimensions of flavor-changing four-quark operators within and beyond the standard model," *Nuclear Physics B* **586** (2000) 397–426, hep-ph/0005183.

[73] F. Gabbiani, E. Gabrielli, A. Masiero, and L. Silvestrini, "A complete analysis of fcnc and cp constraints in general susy extensions of the standard model," *Nuclear Physics B* **477** (1996) 321–352, hep-ph/9604387.

[74] E. E. Jenkins, A. V. Manohar, and P. Stoffer, "Low-energy effective field theory below the electroweak scale: Operators and matching," *Journal of High Energy Physics* **2018** no. 3, (2018) 016, arXiv:1709.04486.

[75] W. Dekens and P. Stoffer, "Low-energy effective field theory below the electroweak scale: matching at one loop," *Journal of High Energy Physics* **2019** no. 10, (2019) 197, arXiv:1908.05295.

[76] M. Pospelov and A. Ritz, "Annals phys. 318 (2005) 119," *Annals of Physics* **318** (2005) 119, hep-ph/0504231.

[77] M. Baak, M. Goebel, J. Haller, A. Hoecker, D. Kennedy, R. Kogler, K. Moenig, M. Schott, and J. Stelzer, "The Electroweak Fit of the Standard Model after the Discovery of a New Boson at the LHC," *Eur. Phys. J. C* **72** (2012) 2205, arXiv:1209.2716 [hep-ph].

[78] M. E. Peskin and T. Takeuchi, "A New constraint on a strongly interacting Higgs sector," *Phys. Rev. Lett.* **65** (1990) 964–967.

[79] M. E. Peskin and T. Takeuchi, "Estimation of oblique electroweak corrections," *Phys. Rev. D* **46** (1992) 381–409.

[80] J. Erler, "Global fits of the SM parameters," *PoS* **LHCP2019** (2019) 105, arXiv:1908.07327 [hep-ph].

[81] H. Fritzsch, "Fundamental constants at high-energy," *Fortsch. Phys.* **50** (2002) 518–524, arXiv:hep-ph/0201198.

[82] V. Sharma, "11. status of higgs boson physics,".

[83] M. Grazzini, A. Ilnicka, and M. Spira, "Higgs boson production at large transverse momentum within the SMEFT: analytical results," *Eur. Phys. J. C* **78** no. 10, (2018) 808, arXiv:1806.08832 [hep-ph].

[84] M. Gillioz, R. Grober, C. Grojean, M. Muhlleitner, and E. Salvioni, "Higgs Low-Energy Theorem (and its corrections) in Composite Models," *JHEP* **10** (2012) 004, arXiv:1206.7120 [hep-ph].